UNIVERSIDAD DE CONCEPCIÓN

Centro de Investigación en Ingeniería Matemática (CI^{2}MA)

A mixed virtual element method for a nonlinear Brinkman model of porous media flow

Gabriel N. Gatica, Mauricio Munar,
Filander A. Sequeira

PREPRINT 2017-32

SERIE DE PRE-PUBLICACIONES

A mixed virtual element method for a nonlinear Brinkman model of porous media flow *

Gabriel N. Gatica† Mauricio Munar‡ Filánder A. Sequeira§

Abstract

In this work we introduce and analyze a mixed virtual element method (mixed VEM) for the two-dimensional nonlinear Brinkman model of porous media flow with non-homogeneous Dirichlet boundary conditions. For the continuous formulation we consider a dual-mixed approach in which the main unknowns are given by the gradient of the velocity and the pseudostress, whereas the velocity itself and the pressure are computed via simple postprocessing formulae. In addition, because of analysis reasons we add a redundant term arising from the constitutive equation relating the pseudostress and the velocity, so that the well-posedness of the resulting augmented formulation is established by using known results from nonlinear functional analysis. Then, we introduce the main features of the mixed virtual element method, which employs an explicit piecewise polynomial subspace and a virtual element subspace for approximating the aforementioned main unknowns, respectively. In turn, the associated computable discrete nonlinear operator is defined in terms of the $\mathbb{L}^2$-orthogonal projector onto a suitable space of polynomials, which allows the explicit integration of the terms involving deviatoric tensors that appear in the original setting. Next, we show the well-posedness of the discrete scheme and derive the associated a priori error estimates for the virtual element solution as well as for the fully computable projection of it. Furthermore, we also introduce a second element-by-element postprocessing formula for the pseudostress, which yields an optimally convergent approximation of this unknown with respect to the broken $\mathbb{H}(\mathbf{div})$-norm. Finally, several numerical results illustrating the good performance of the method and confirming the theoretical rates of convergence are presented.

Key words: nonlinear Brinkman model, augmented formulation, virtual element method, a priori error analysis, postprocessing techniques, high-order approximations

Mathematical subject classifications (2000): 65N30, 65N12, 65N15.

1 Introduction

The numerical solution of diverse linear and nonlinear boundary value problems in fluid mechanics by means of the VEM technique has become a very promising research subject during recent years. In fact, we first refer to [2], [6], and [16], where several virtual element methods, including stream

*This work was partially supported by CONICYT-Chile through BASAL project CMM, Universidad de Chile, and the Becas-CONICYT Programme for foreign students; by Centro de Investigación en Ingeniería Matemática (CI^{2}MA), Universidad de Concepción; and by Universidad Nacional (Costa Rica), through the project 0106-16.

†CI^{2}MA and Departamento de Ingeniería Matemática, Universidad de Concepción, Casilla 160-C, Concepción, Chile, email: ggatica@ci2ma.udec.cl.

‡CI^{2}MA and Departamento de Ingeniería Matemática, Universidad de Concepción, Casilla 160-C, Concepción, Chile, email: mmunar@ci2ma.udec.cl.

§Escuela de Matemática, Universidad Nacional, Campus Omar Dengo, Heredia, Costa Rica, email: filander.sequeira@una.cr.

function-based, divergence free, and non-conforming schemes, have been proposed for the classical velocity-pressure formulation of the Stokes equation. In turn, the method from [6] has been recently extended in [7] to the two-dimensional Navier-Stokes equations, thus yielding, up to our knowledge, the first VEM approach for this nonlinear model. On the other hand, and concerning the use of *dual-mixed* formulations, that is those in which the main unknown usually lives in either a vectorial $\mathbf{H}(\mathrm{div})$ or a tensorial $\mathbb{H}(\mathbf{div})$ space, we remark that several contributions have concentrated on the combination of VEM and pseudostress-based approaches, being the latter motivated by the need of circumventing the symmetry requirement of the usual stress-based methods. In particular, a mixed-VEM for the pseudostress-velocity formulation of the Stokes problem, in which the pressure is computed via a postprocessing formula, was introduced in [10]. The analysis in [10] is then extended in [12] to derive two mixed virtual element methods for the two-dimensional Brinkman problem. An interesting feature of both schemes in [12] refers to their robustness as the Stokes limit of the Brinkman model is approached. The corresponding pseudostress-based dual-mixed finite element methods for this model and its nonlinear version had been previously developed in [17] and [18], respectively. In addition, the approach from [10] and [12] was extended in [11] to the case of quasi-Newtonian Stokes flows. More precisely, a virtual element method for an augmented mixed variational formulation of the class of nonlinear Stokes models studied in [22] (see also [24], [25]) is introduced and analyzed in [11]. Furthermore, in the recent work [23] we considered the same variational formulation from [15] (see also [13], [14]) and proposed, up to our knowledge, the first dual-mixed virtual element method for the Navier Stokes equations. Indeed, the approach employed in [23] is based on the introduction of a nonlinear pseudostress linking the convective term with the usual pseudostress for the Stokes equations. We end this paragraph by highlighting that, besides the basic principles of the VEM philosophy (cf. [3] and [8]), most of the aforedescribed works on mixed VEM for pseudostress-based variational formulations have made extensive use of the key contributions provided in [1], [4], and [5]. In particular, the exact computations of the L^2-projections onto suitable spaces of polynomials have certainly enriched the potential applications of the H^1 and H(div) conforming cases.

According to the foregoing discussion, and in order to continue developing pseudostrees-based mixed virtual element methods for nonlinear models in fluid mechanics, we now aim to extend the analysis and results from [11] and [23] to the case of the problem studied in [18]. In other words, the purpose of the present paper is to extend the analysis and results from [12] to a class of Brinkman models whose viscosity depends nonlinearly on the gradient of the velocity, which is a characteristic feature of quasi-Newtonian Stokes flows (see, e.g. [21, 22, 25, 26]). In order to deal with the aforedescribed nonlinearity, we follow [18] and introduce the gradient of the velocity as a new unknown. Moreover, we modify the resulting variational formulation by augmenting it with a redundant equation arising from the constitutive law relating the pseudostress and the velocity gradient, which allows us to apply known results from nonlinear functional analysis.

The rest of this work is organized as follows. In Section 2 we define the boundary value problem of interest, introduce its pseudostress-based mixed formulation, and provide the associated well-posedness result. Next, in Section 3 we follow [4] and [5] to introduce the virtual element subspace that will be employed. This includes the basic assumptions on the polygonal mesh, the definition of the local virtual element space, and the projections and interpolants to be utilized together with their respective approximation properties. Further, we introduce a fully calculable local discrete nonlinear operator. Then, we set the corresponding mixed virtual element method, and apply the classical theory of nonlinear operators to conclude its well-posedness. In turn, in Section 4 we employ suitable bounds and identities satisfied by the nonlinear operator and the projectors and interpolators involved, to derive the a priori error estimates and corresponding rates of convergence for the virtual solution as well as for the computable projection of it. In addition, we follow the ideas from [19] and [20] to construct a second approximation for the pseudostress variable $\boldsymbol{\sigma}$, which yields an optimal rate of convergence in the broken H(div)-norm. We remark that this new postprocessing formula can be

used in general for any H(div)-conforming VEM scheme. Finally, several numerical examples showing the good performance of the method, confirming the rates of convergence for regular and singular solutions, and illustrating the accurateness obtained with the approximate solutions, are reported in Section 5.

We end this section with several notations to be used throughout the paper. Firstly, we let $\mathbb{I}$ be the identity matrix in $\mathrm{R}^{2\times 2}$, and for any $\boldsymbol{\tau} := (\tau_{ij})$, $\boldsymbol{\zeta} := (\zeta_{ij}) \in \mathrm{R}^{2\times 2}$, we set

$$\boldsymbol{\tau}^{\mathbf{t}} := (\tau_{ji}), \quad \mathrm{tr}(\boldsymbol{\tau}) := \sum_{i=1}^{2} \tau_{ii}, \quad \boldsymbol{\tau}^{\mathbf{d}} := \boldsymbol{\tau} - \frac{1}{2}\mathrm{tr}(\boldsymbol{\tau})\,\mathbb{I}, \quad \text{and} \quad \boldsymbol{\tau} : \boldsymbol{\zeta} := \sum_{i,j=1}^{2} \tau_{ij}\zeta_{ij},$$

which denote, respectively, the transpose, the trace, and the deviator of the tensor $\boldsymbol{\tau}$, and the tensorial product between $\boldsymbol{\tau}$ and $\boldsymbol{\zeta}$. Next, given a bounded domain $\mathcal{O} \subseteq \mathrm{R}^2$, with polygonal boundary $\partial\mathcal{O}$, we utilize standard notations for Lebesgue spaces $\mathrm{L}^p(\mathcal{O})$, $p > 1$, and Sobolev spaces $\mathrm{H}^s(\mathcal{O})$, $s \in \mathrm{R}$, with norm $\|\cdot\|_{s,\mathcal{O}}$ and seminorm $|\cdot|_{s,\mathcal{O}}$. In particular, $\mathrm{H}^{1/2}(\partial\mathcal{O})$ is the space of traces of functions of $\mathrm{H}^1(\mathcal{O})$ and $\mathrm{H}^{-1/2}(\partial\mathcal{O})$ denotes its dual. Moreover, by $\mathbf{M}$ and $\mathbb{M}$ we will refer to the corresponding vector and tensorial counterparts of the generic scalar functional space M, and $\|\cdot\|$, with no subscripts, will stand for the natural norm of either an element or an operator in any product functional space. Furthermore, we recall that

$$\mathbb{H}(\mathbf{div};\mathcal{O}) := \left\{ \boldsymbol{\tau} \in \mathbb{L}^2(\mathcal{O}) : \quad \mathbf{div}(\boldsymbol{\tau}) \in \mathbf{L}^2(\mathcal{O}) \right\},$$

equipped with the usual norm

$$\|\boldsymbol{\tau}\|^2_{\mathbf{div};\mathcal{O}} := \|\boldsymbol{\tau}\|^2_{0,\mathcal{O}} + \|\mathbf{div}(\boldsymbol{\tau})\|^2_{0,\mathcal{O}} \qquad \forall\, \boldsymbol{\tau} \in \mathbb{H}(\mathbf{div};\mathcal{O}),$$

is a Hilbert space. Finally, we employ $\mathbf{0}$ to denote a generic null vector, null tensor or null operator, and use C and c, with or without subscripts to denote generic constants independent of the discretization parameters, which may take different values at different places.

2 The continuous problem

2.1 The model problem

Let Ω be a bounded domain in R^2 with polygonal boundary Γ. Given a volume force $\mathbf{f} \in \mathbf{L}^2(\Omega)$ and a Dirichlet datum $\mathbf{g} \in \mathbf{H}^{1/2}(\Gamma)$, we seek a tensor $\boldsymbol{\sigma}$ (pseudostress), a vector field $\mathbf{u}$ (velocity), and a scalar field p (pressure), such that

$$\begin{aligned} &\boldsymbol{\sigma} = \mu(|\nabla\mathbf{u}|)\nabla\mathbf{u} - p\,\mathbb{I} \quad \text{in} \quad \Omega\,, \quad \alpha\mathbf{u} - \mathbf{div}(\boldsymbol{\sigma}) = \mathbf{f} \quad \text{in} \quad \Omega\,, \\ &\mathrm{div}(\mathbf{u}) = 0 \quad \text{in} \quad \Omega\,, \quad \mathbf{u} = \mathbf{g} \quad \text{on} \quad \Gamma\,, \quad \text{and} \quad \int_\Omega p = 0\,, \end{aligned} \tag{2.1}$$

where $\mu : \mathrm{R}^+ \to \mathrm{R}$ is the nonlinear kinematic viscosity function of the fluid, and $\alpha > 0$ is a constant approximation of the viscosity divided by the permeability. In addition, note according to the incompressibility of the fluid, that $\mathbf{g}$ must satisfy the compatibility condition $\int_\Gamma \mathbf{g}\cdot\boldsymbol{\nu} = 0$, where $\boldsymbol{\nu}$ is the unit outward normal on Γ, and that the uniqueness of a pressure solution is ensured by the last equation of (2.1).

In what follows, we let $\mu_{ij} : \mathrm{R}^{2\times 2} \to \mathrm{R}$ be the mapping given by $\mu_{ij} := \mu(|\mathbf{r}|)r_{ij}$ for each $\mathbf{r} := (r_{ij}) \in \mathrm{R}^{2\times 2}$ and for each $i, j \in \{1, 2\}$. Then, throughout this paper we assume that μ is of class C^1 and that there exist $\gamma_0, \alpha_0 > 0$ such that for each $\mathbf{r} := (r_{ij}), \mathbf{s} := (s_{ij}) \in \mathrm{R}^{2\times 2}$, there hold

$$|\mu_{ij}(\mathbf{r})| \leq \gamma_0|\mathbf{r}|, \quad \text{and} \quad \left|\frac{\partial}{\partial r_{kl}}\mu_{ij}(\mathbf{r})\right| \leq \gamma_0 \quad \forall\, i, j, k, l \in \{1, 2\}, \tag{2.2}$$

and

$$\sum_{i,j,k,l=1}^{2} \frac{\partial}{\partial r_{kl}} \mu_{ij}(\mathbf{r}) s_{ij} s_{kl} \geq \alpha_0 |\mathbf{s}|^2. \tag{2.3}$$

A classical example of nonlinear functions μ is given by the well-known Carreau law in fluid mechanics (see e.g. [27, 28])

$$\mu(s) \ := \ \rho_0 + \rho_1 (1 + s^2)^{(\beta-2)/2} \qquad \forall \ s \geq 0, \tag{2.4}$$

where $\rho_0, \rho_1 > 0$ and $\beta > 1$. In particular, note that with $\beta = 2$ we recover the usual linear Brinkman model. It is easy to check that (2.4) satisfies the assumptions (2.2) and (2.3) for all $\rho_0, \rho_1 > 0$ and for all $\beta \in [1, 2]$, with

$$\gamma_0 = \rho_0 + \rho_1 \left\{ \frac{|\beta - 2|}{2} + 1 \right\} \quad \text{and} \quad \alpha_0 = \rho_0. \tag{2.5}$$

2.2 The continuous formulation

Here we proceed as in [18] to derive a weak formulation for (2.1). In fact, we begin by observing that the first equation of (2.1) together with the incompressibility condition are equivalent to the pair of equations given by

$$\boldsymbol{\sigma}^{\mathbf{d}} = \mu(|\nabla \mathbf{u}|) \nabla \mathbf{u} \quad \text{in} \quad \Omega \quad \text{and} \quad p = -\frac{1}{2} \mathrm{tr}(\boldsymbol{\sigma}) \quad \text{in} \quad \Omega, \tag{2.6}$$

whence introducing the auxiliary unknown $\mathbf{t} := \nabla \mathbf{u}$ in Ω, we can rewrite (2.1) as follows:

$$\begin{gathered} \mathbf{t} = \nabla \mathbf{u} \quad \text{in} \quad \Omega, \quad \boldsymbol{\sigma}^{\mathbf{d}} = \mu(|\mathbf{t}|)\mathbf{t} \quad \text{in} \quad \Omega\,, \qquad \alpha \mathbf{u} - \mathbf{div}(\boldsymbol{\sigma}) \ = \ \mathbf{f} \quad \text{in} \quad \Omega\,, \\ \mathrm{tr}(\mathbf{t}) = \mathbf{0} \quad \text{in} \quad \Omega\,, \quad \mathbf{u} = \ \mathbf{g} \quad \text{on} \quad \Gamma\,, \quad \text{and} \quad \int_\Omega \mathrm{tr}(\boldsymbol{\sigma}) = 0\,. \end{gathered} \tag{2.7}$$

In this way, we notice from the fourth and last equation of (2.7) that the unknowns $\mathbf{t}$ and $\boldsymbol{\sigma}$ live in the spaces

$$\mathbb{L}^2_{\mathrm{tr}}(\Omega) \ := \ \left\{ \mathbf{s} \in \mathbb{L}^2(\Omega) : \quad \mathrm{tr}(\mathbf{s}) = 0 \right\},$$

and

$$\mathbb{H}_0(\mathbf{div}; \Omega) \ := \ \left\{ \boldsymbol{\zeta} \in \mathbb{H}(\mathbf{div}; \Omega) : \quad \int_\Omega \mathrm{tr}(\boldsymbol{\zeta}) = 0 \right\},$$

respectively. Then, testing the first and second equation of (2.7) with $\boldsymbol{\tau} \in \mathbb{H}_0(\mathbf{div}; \Omega)$ and $\mathbf{s} \in \mathbb{L}^2_{\mathrm{tr}}(\Omega)$, respectively, integrating by parts, using the Dirichlet condition for $\mathbf{u}$, and denoting by $\langle \cdot, \cdot \rangle$ the duality pairing between $\mathbf{H}^{-1/2}(\Gamma)$ and $\mathbf{H}^{1/2}(\Gamma)$, we arrive at

$$\int_\Omega \mu(|\mathbf{t}|) \mathbf{t} : \mathbf{s} - \int_\Omega \mathbf{s} : \boldsymbol{\sigma}^{\mathbf{d}} = 0 \qquad \forall \ \mathbf{s} \in \mathbb{L}^2_{\mathrm{tr}}(\Omega)\,, \tag{2.8}$$

and

$$\int_\Omega \mathbf{t} : \boldsymbol{\tau}^{\mathbf{d}} + \int_\Omega \mathbf{u} \cdot \mathbf{div}(\boldsymbol{\tau}) = \langle \boldsymbol{\tau} \boldsymbol{\nu}, \mathbf{g} \rangle \qquad \forall \ \boldsymbol{\tau} \in \mathbb{H}_0(\mathbf{div}; \Omega)\,, \tag{2.9}$$

where we used the fact that $\mathbf{t} = \mathbf{t}^{\mathbf{d}}$, which implies the equality $\int_\Omega \mathbf{t} : \boldsymbol{\tau} = \int_\Omega \mathbf{t} : \boldsymbol{\tau}^{\mathbf{d}}$. In turn, the velocity is replaced from the third equation of (2.7), that is

$$\mathbf{u} \ = \ \frac{1}{\alpha} \left\{ \mathbf{f} \ + \ \mathbf{div}(\boldsymbol{\sigma}) \right\} \quad \text{in} \quad \Omega\,, \tag{2.10}$$

whence (2.9) becomes

$$\int_\Omega \mathbf{t} : \boldsymbol{\tau}^{\mathbf{d}} \ + \ \frac{1}{\alpha} \int_\Omega \mathbf{div}(\boldsymbol{\sigma}) \cdot \mathbf{div}(\boldsymbol{\tau}) \ = \ -\frac{1}{\alpha} \int_\Omega \mathbf{f} \cdot \mathbf{div}(\boldsymbol{\tau}) + \langle \boldsymbol{\tau} \boldsymbol{\nu}, \mathbf{g} \rangle \qquad \forall \ \boldsymbol{\tau} \in \mathbb{H}_0(\mathbf{div}; \Omega)\,.$$

The foregoing equation together with (2.8) yield at first instance the following variational formulation of (2.7): Find $\mathbf{t} \in X := \mathbb{L}^2_{\mathrm{tr}}(\Omega)$ and $\boldsymbol{\sigma} \in H := \mathbb{H}_0(\mathbf{div};\Omega)$ such that

$$\begin{array}{rcll} \displaystyle\int_\Omega \mu(|\mathbf{t}|)\mathbf{t} : \mathbf{s} - \int_\Omega \mathbf{s} : \boldsymbol{\sigma}^{\mathbf{d}} & = & 0 & \forall\, \mathbf{s} \in X\,, \\ \displaystyle\int_\Omega \mathbf{t} : \boldsymbol{\tau}^{\mathbf{d}} + \frac{1}{\alpha}\int_\Omega \mathbf{div}(\boldsymbol{\sigma}) \cdot \mathbf{div}(\boldsymbol{\tau}) & = & \displaystyle -\frac{1}{\alpha}\int_\Omega \mathbf{f} \cdot \mathbf{div}(\boldsymbol{\tau}) + \langle \boldsymbol{\tau}\boldsymbol{\nu}, \mathbf{g}\rangle & \forall\, \boldsymbol{\tau} \in H\,. \end{array} \tag{2.11}$$

However, in order to analyse the solvability of (2.11), we need to perform a suitable modification of it. More precisely, given a stabilization parameter $\kappa > 0$ to be suitably chosen later on, we incorporate into (2.11) the following redundant Galerkin term:

$$\kappa \int_\Omega \Big\{ \boldsymbol{\sigma}^{\mathbf{d}} - \mu(|\mathbf{t}|)\mathbf{t} \Big\} : \boldsymbol{\tau}^{\mathbf{d}} \;=\; 0 \qquad \forall\, \boldsymbol{\tau} \in \mathbb{H}_0(\mathbf{div};\Omega)\,,$$

which leads to the augmented formulation: Find $(\mathbf{t}, \boldsymbol{\sigma}) \in X \times H$ such that

$$[\mathbf{A}(\mathbf{t}, \boldsymbol{\sigma}), (\mathbf{s}, \boldsymbol{\tau})] \;=\; [\mathbf{F}, (\mathbf{s}, \boldsymbol{\tau})] \qquad \forall\, (\mathbf{s}, \boldsymbol{\tau}) \in X \times H\,, \tag{2.12}$$

where $[\cdot,\cdot]$ stands for the duality pairing between $(X \times H)'$ and $X \times H$, $\mathbf{A} : X \times H \to (X \times H)'$ is the nonlinear operator

$$\begin{array}{rl} [\mathbf{A}(\mathbf{r}, \boldsymbol{\zeta}), (\mathbf{s}, \boldsymbol{\tau})] \;:=\; \displaystyle\int_\Omega \mu(|\mathbf{r}|)\mathbf{r} : \mathbf{s} - \int_\Omega \mathbf{s} : \boldsymbol{\zeta}^{\mathbf{d}} \;+\; \int_\Omega \mathbf{r} : \boldsymbol{\tau}^{\mathbf{d}} \\ \quad + \;\kappa \displaystyle\int_\Omega \Big\{ \boldsymbol{\zeta}^{\mathbf{d}} - \mu(|\mathbf{r}|)\mathbf{r} \Big\} : \boldsymbol{\tau}^{\mathbf{d}} \;+\; \frac{1}{\alpha}\int_\Omega \mathbf{div}(\boldsymbol{\zeta}) \cdot \mathbf{div}(\boldsymbol{\tau})\,, \end{array} \tag{2.13}$$

and $\mathbf{F} : X \times H \to \mathrm{R}$ is the bounded linear functional

$$[\mathbf{F}, (\mathbf{s}, \boldsymbol{\tau})] \;:=\; -\frac{1}{\alpha}\int_\Omega \mathbf{f} \cdot \mathbf{div}(\boldsymbol{\tau}) \;+\; \langle \boldsymbol{\tau}\boldsymbol{\nu}, \mathbf{g}\rangle, \tag{2.14}$$

for all $(\mathbf{r}, \boldsymbol{\zeta}), (\mathbf{s}, \boldsymbol{\tau}) \in X \times H$. In addition, we also observe that we can write

$$\begin{array}{rl} [\mathbf{A}(\mathbf{r}, \boldsymbol{\zeta}), (\mathbf{s}, \boldsymbol{\tau})] \;:=\; [\mathbb{A}(\mathbf{r}), \mathbf{s} - \kappa\boldsymbol{\tau}^{\mathbf{d}}] \;-\; \displaystyle\int_\Omega \mathbf{s} : \boldsymbol{\zeta}^{\mathbf{d}} \;+\; \int_\Omega \mathbf{r} : \boldsymbol{\tau}^{\mathbf{d}} \\ \quad + \;\kappa \displaystyle\int_\Omega \boldsymbol{\zeta}^{\mathbf{d}} : \boldsymbol{\tau}^{\mathbf{d}} \;+\; \frac{1}{\alpha}\int_\Omega \mathbf{div}(\boldsymbol{\zeta}) \cdot \mathbf{div}(\boldsymbol{\tau})\,, \end{array} \tag{2.15}$$

for each $(\mathbf{r}, \boldsymbol{\zeta}), (\mathbf{s}, \boldsymbol{\tau}) \in X \times H$, where $\mathbb{A} : X \to X'$ is the auxiliary nonlinear operator defined by

$$[\mathbb{A}(\mathbf{r}), \mathbf{s}] \;:=\; \int_\Omega \mu(|\mathbf{r}|)\mathbf{r} : \mathbf{s} \qquad \forall\, \mathbf{r}, \mathbf{s} \in X.$$

At this point we recall from [22, Lemma 2.1] that $\mathbb{A}$ is Lipschitz-continuous and strongly monotone, that is, with the constants γ_0 and α_0 specified in (2.2) and (2.3), respectively, there hold

$$\|\mathbb{A}(\mathbf{r}) - \mathbb{A}(\mathbf{s})\|_{X'} \;\leq\; \gamma_0 \|\mathbf{r} - \mathbf{s}\|_{0,\Omega}\,, \tag{2.16}$$

and

$$[\mathbb{A}(\mathbf{r}) - \mathbb{A}(\mathbf{s}), \mathbf{r} - \mathbf{s}] \;\geq\; \alpha_0 \|\mathbf{r} - \mathbf{s}\|^2_{0,\Omega}\,, \tag{2.17}$$

for each $\mathbf{r}, \mathbf{s} \in X$. In addition, employing the Cauchy-Schwarz inequality and the estimate (2.16), we deduce from (2.15) that $\mathbf{A}$ is Lipschitz-continuous with constant $L_{\mathbf{A}} := \max\{1, \kappa, \gamma_0, \frac{1}{\alpha}\}$, that is

$$\| \mathbf{A}(\mathbf{t}, \boldsymbol{\sigma}) - \mathbf{A}(\mathbf{r}, \boldsymbol{\zeta}) \|_{(X\times H)'} \;\leq\; L_{\mathbf{A}}\, \|(\mathbf{t}, \boldsymbol{\sigma}) - (\mathbf{r}, \boldsymbol{\zeta})\|_{X\times H} \qquad \forall\, (\mathbf{t}, \boldsymbol{\sigma}),\, (\mathbf{r}, \boldsymbol{\zeta}) \,\in\, X \times H\,. \tag{2.18}$$

Moreover, in what follows we show that $\mathbf{A}$ is strongly monotone as well. For this purpose, we need the following technical result.

Lemma 2.1. *There exists $c(\Omega) > 0$, depending only on Ω, such that*

$$c(\Omega)\,\|\boldsymbol{\tau}\|_{0,\Omega}^2 \;\leq\; \|\boldsymbol{\tau}^{\mathbf{d}}\|_{0,\Omega}^2 \;+\; \|\mathbf{div}(\boldsymbol{\tau})\|_{0,\Omega}^2 \qquad \forall\, \boldsymbol{\tau} \in H.$$

Proof. See [9, Chapter IV, Proposition 3.1] □

Then, the announced result on $\mathbf{A}$ is established as follows.

Lemma 2.2. *Let $\mathbf{A}$ be the nonlinear operator defined in* (2.13)*. Assume that, given $\delta \in \left(0, \dfrac{2}{\gamma_0}\right)$, the parameter κ lies in $\left(0, \dfrac{2\delta\alpha_0}{\gamma_0}\right)$. Then, there exists a positive constant C_{SM}, independent of h, such that for all $(\mathbf{r},\boldsymbol{\zeta}), (\mathbf{s},\boldsymbol{\tau}) \in X \times H$ there holds*

$$[\mathbf{A}(\mathbf{r},\boldsymbol{\zeta}) - \mathbf{A}(\mathbf{s},\boldsymbol{\tau}), (\mathbf{r},\boldsymbol{\zeta}) - (\mathbf{s},\boldsymbol{\tau})] \;\geq\; C_{SM}\|(\mathbf{r},\boldsymbol{\zeta}) - (\mathbf{s},\boldsymbol{\tau})\|_{X\times H}^2.$$

Proof. Given $(\mathbf{r},\boldsymbol{\zeta}), (\mathbf{s},\boldsymbol{\tau}) \in X \times H$, we obtain from (2.15) that

$$\begin{aligned}[\mathbf{A}(\mathbf{r},\boldsymbol{\zeta}) - \mathbf{A}(\mathbf{s},\boldsymbol{\tau}), (\mathbf{r},\boldsymbol{\zeta}) - (\mathbf{s},\boldsymbol{\tau})] \;&=\; [\mathbb{A}(\mathbf{r}) - \mathbb{A}(\mathbf{s}), \mathbf{r} - \mathbf{s}] \\ &- \kappa\,[\mathbb{A}(\mathbf{r}) - \mathbb{A}(\mathbf{s}), (\boldsymbol{\zeta} - \boldsymbol{\tau})^{\mathbf{d}}] \;+\; \kappa\,\|(\boldsymbol{\zeta} - \boldsymbol{\tau})^{\mathbf{d}}\|_{0,\Omega}^2 \;+\; \frac{1}{\alpha}\,\|\mathbf{div}(\boldsymbol{\zeta} - \boldsymbol{\tau})\|_{0,\Omega}^2\,,\end{aligned}$$

from which, using the Cauchy-Schwarz and Young inequalities, the Lipschitz-continuity and strong monotonicity properties of the operator $\mathbb{A}$, and Lemma 2.1, we find that

$$\begin{aligned}&[\mathbf{A}(\mathbf{r},\boldsymbol{\zeta}) - \mathbf{A}(\mathbf{s},\boldsymbol{\tau}), (\mathbf{r},\boldsymbol{\zeta}) - (\mathbf{s},\boldsymbol{\tau})] \\ &\geq\; \left(\alpha_0 - \frac{\kappa\gamma_0}{2\delta}\right)\|\mathbf{r} - \mathbf{s}\|_{0,\Omega}^2 \;+\; \kappa\,\left(1 - \frac{\gamma_0\delta}{2}\right)\,\|(\boldsymbol{\zeta} - \boldsymbol{\tau})^{\mathbf{d}}\|_{0,\Omega}^2 \;+\; \frac{1}{\alpha}\,\|\mathbf{div}(\boldsymbol{\zeta} - \boldsymbol{\tau})\|_{0,\Omega}^2 \\ &\geq\; \left(\alpha_0 - \frac{\kappa\gamma_0}{2\delta}\right)\|\mathbf{r} - \mathbf{s}\|_{0,\Omega}^2 \;+\; c(\Omega)\,\min\left\{\kappa\,\left(1 - \frac{\gamma_0\delta}{2}\right), \frac{1}{2\alpha}\right\}\|\boldsymbol{\zeta} - \boldsymbol{\tau}\|_{0,\Omega}^2 \;+\; \frac{1}{2\alpha}\|\mathbf{div}(\boldsymbol{\zeta} - \boldsymbol{\tau})\|_{0,\Omega}^2\,.\end{aligned}$$

Finally, it suffices to choose $C_{SM} := \min\left\{\left(\alpha_0 - \dfrac{\kappa\gamma_0}{2\delta}\right), c(\Omega)\,\min\left\{\kappa\,\left(1 - \dfrac{\gamma_0\delta}{2}\right), \dfrac{1}{2\alpha}\right\}, \dfrac{1}{2\alpha}\right\}$. □

Hence, the well-posedness of the variational formulation (2.12) is provided by the following theorem.

Theorem 2.1. *Assume that $\mathbf{f} \in \mathbf{L}^2(\Omega), \mathbf{g} \in \mathbf{H}^{1/2}(\Gamma)$, and that the parameter κ satisfy the conditions required by* Lemma 2.2*. Then, there exists a unique $(\mathbf{t},\boldsymbol{\sigma}) \in X \times H$ solution of* (2.12)*. Moreover, there exists a positive constant C, depending only on $\Omega, \alpha_0, \gamma_0, \kappa$ and α, such that*

$$\|(\mathbf{t},\boldsymbol{\sigma})\|_{X\times H} \;\leq\; C\left\{\|\mathbf{f}\|_{0,\Omega} \;+\; \|\mathbf{g}\|_{1/2,\Gamma}\right\}.$$

Proof. Thanks to the Lipschitz-continuity and the strong monotonicity of the operator $\mathbf{A}$, the proof is a straightforward application of [29, Theorem 25.B]. □

3 The mixed virtual element method

In this section we introduce and analyze a mixed virtual element scheme for the continuous formulation (2.12). An explicit piecewise polynomial subspace and a suitable virtual element subspace are employed for approximating $\mathbf{t} \in X$ and $\boldsymbol{\sigma} \in H$, respectively. While all the definitions and results concerning the latter subspace, including its associated interpolation operator and main approximation properties, are available in [5] and [11], most of the corresponding details are recalled in what follows for convenience of the reader. We begin with some preliminaries.

3.1 Preliminaries

Let $\{\mathcal{T}_h\}_{h>0}$ be a family of decompositions of Ω in polygonal elements. Then, for each $K \in \mathcal{T}_h$ we denote its diameter by h_K, and define, as usual, $h := \max\{h_K : K \in \mathcal{T}_h\}$. Furthermore, in what follows we assume that there exists a constant $C_{\mathcal{T}} > 0$ such that for each decomposition $\mathcal{T}_h$ and for each $K \in \mathcal{T}_h$ there hold:

a) the ratio between the shortest edge and the diameter h_K of K is bigger than $C_{\mathcal{T}}$, and

b) K is star-shaped with respect to a ball B of radius $C_{\mathcal{T}} h_K$ and center $\mathbf{x}_B \in K$.

We recall here that, as consequence of the above hypotheses, one can show that each $K \in \mathcal{T}_h$ is simply connected, and that there exists an integer $N_{\mathcal{T}}$ (depending only on $C_{\mathcal{T}}$), such that the number of edges of each $K \in \mathcal{T}_h$ is bounded above by $N_{\mathcal{T}}$.

Now, given an integer $\ell \geq 0$ and $\mathcal{O} \subseteq \mathrm{R}^2$, we let $\mathrm{P}_\ell(\mathcal{O})$ be the space of polynomials on $\mathcal{O}$ of degree up to ℓ, and according to Section 1, we set $\mathbf{P}_\ell(\mathcal{O}) := [\mathrm{P}_\ell(\mathcal{O})]^2$ and $\mathbb{P}_\ell(\mathcal{O}) := [\mathrm{P}_\ell(\mathcal{O})]^{2\times 2}$. Furthermore, given an edge e of $\mathcal{T}_h$ with barycentric x_e and diameter h_e, we introduce the following set of $(\ell+1)$ normalized monomials on e

$$\mathcal{B}_\ell(e) \ := \ \left\{ \left(\frac{x - x_e}{h_e} \right)^j \right\}_{0 \leq j \leq \ell},$$

which certainly constitutes a basis on $\mathrm{P}_\ell(e)$. Similarly, given $K \in \mathcal{T}_h$ with barycenter $\mathbf{x}_K$, we define the following set of $\frac{1}{2}(\ell+1)(\ell+2)$ normalized monomials

$$\mathcal{B}_\ell(K) \ := \ \left\{ \left(\frac{\mathbf{x} - \mathbf{x}_K}{h_K} \right)^{\boldsymbol{\alpha}} \right\}_{0 \leq |\boldsymbol{\alpha}| \leq \ell},$$

which is a basis of $\mathrm{P}_\ell(K)$. Notice that in the definition of $\mathcal{B}_\ell(K)$ above, we have made use of the multi-index notation, that is, given $\mathbf{x} := (x_1, x_2)^{\mathbf{t}} \in \mathrm{R}^2$ and $\boldsymbol{\alpha} := (\alpha_1, \alpha_2)^{\mathbf{t}}$, with non-negative integers α_1, α_2, we set $\mathbf{x}^{\boldsymbol{\alpha}} := x_1^{\alpha_1} x_2^{\alpha_2}$ and $|\boldsymbol{\alpha}| := \alpha_1 + \alpha_2$. Furthermore, for e and K as indicated, we define

$$\boldsymbol{\mathcal{B}}_\ell(e) \ := \ \Big\{ (q,0)^{\mathbf{t}} \ : \ q \in \mathcal{B}_\ell(e) \Big\} \cup \Big\{ (0,q)^{\mathbf{t}} \ : \ q \in \mathcal{B}_\ell(e) \Big\},$$

and

$$\boldsymbol{\mathcal{B}}_\ell(K) \ := \ \Big\{ (q,0)^{\mathbf{t}} \ : \ q \in \mathcal{B}_\ell(K) \Big\} \ \cup \ \Big\{ (0,q)^{\mathbf{t}} \ : \ q \in \mathcal{B}_\ell(K) \Big\}.$$

On the other hand, for each integer $\ell \geq 0$, we let $\mathcal{G}_\ell(K)$ be a basis of $\big(\nabla \mathrm{P}_{\ell+1}(K)\big)^\perp \cap \mathbf{P}_\ell(K)$, which is the $\mathbf{L}^2(K)$-orthogonal of $\nabla \mathrm{P}_{\ell+1}(K)$ in $\mathbf{P}_\ell(K)$, and denote its tensorial counterpart as follows:

$$\boldsymbol{\mathcal{G}}_\ell(K) \ := \ \left\{ \begin{pmatrix} \mathbf{q} \\ \mathbf{0} \end{pmatrix} \ : \ \mathbf{q} \in \mathcal{G}_\ell(K) \right\} \cup \left\{ \begin{pmatrix} \mathbf{0} \\ \mathbf{q} \end{pmatrix} \ : \ \mathbf{q} \in \mathcal{G}_\ell(K) \right\}.$$

3.2 The virtual element spaces and its approximation properties

Given an integer $k \geq 0$, we define the finite dimensional subspaces of X and H, respectively, as

$$X_k^h \ := \ \big\{ \mathbf{s} \in X : \quad \mathbf{s}\big|_K \in X_k^K \quad \forall\, K \in \mathcal{T}_h \big\} \tag{3.1}$$

and

$$H_k^h \ := \ \big\{ \boldsymbol{\tau} \in H : \quad \boldsymbol{\tau}\big|_K \in H_k^K \quad \forall\, K \in \mathcal{T}_h \big\}, \tag{3.2}$$

where, given $K \in \mathcal{T}_h$, $X_k^K := \mathbb{P}_k(K)$ and H_k^K is the space introduced in [5, Section 3.1], namely

$$H_k^K := \Big\{ \boldsymbol{\tau} \in \mathbb{H}(\mathbf{div}; K) \cap \mathbb{H}(\mathbf{rot}; K) : \quad \boldsymbol{\tau}\boldsymbol{\nu}|_e \in \mathbf{P}_k(e) \quad \forall \text{ edge } e \in \partial K \,, \\ \mathbf{div}(\boldsymbol{\tau}) \in \mathbf{P}_k(K) \quad \text{and} \quad \mathbf{rot}(\boldsymbol{\tau}) \in \mathbf{P}_{k-1}(K) \Big\} \,. \tag{3.3}$$

The degrees of freedom guaranteeing unisolvency for each $\boldsymbol{\tau} \in H_k^K$ are defined by (see e.g. [4, Section 3.6], [5], [12])

$$\begin{aligned} &\int_e \boldsymbol{\tau}\boldsymbol{\nu} \cdot \mathbf{q} && \forall\, \mathbf{q} \in \boldsymbol{\mathcal{B}}_k(e) \,, \quad \forall \text{ edge } e \in \partial K \,, \\ &\int_K \boldsymbol{\tau} : \nabla \mathbf{p} && \forall\, \mathbf{p} \in \boldsymbol{\mathcal{B}}_k(K) \setminus \{(1,0)^{\mathbf{t}}, (0,1)^{\mathbf{t}}\} \,, \\ &\int_K \boldsymbol{\tau} : \boldsymbol{\rho} && \forall\, \boldsymbol{\rho} \in \boldsymbol{\mathcal{G}}_k(K) \,. \end{aligned} \tag{3.4}$$

In turn, we let $\mathcal{P}_k^K : \mathbf{L}^2(K) \to \mathbf{P}_k(K)$ and $\boldsymbol{\mathcal{P}}_k^K : \mathbb{L}^2(K) \to \mathbb{P}_k(K)$ be the orthogonal projectors. Then, for each integer $m \in \{0, 1, ..., k+1\}$ there hold the following approximation properties:

$$\|\mathbf{v} - \mathcal{P}_k^K(\mathbf{v})\|_{0,K} \;\leq\; C h_K^m |\mathbf{v}|_{m,K} \qquad \forall\, \mathbf{v} \in \mathbf{H}^m(K) \,, \tag{3.5}$$

and

$$\|\boldsymbol{\tau} - \boldsymbol{\mathcal{P}}_k^K(\boldsymbol{\tau})\|_{0,K} \;\leq\; C h_K^m |\boldsymbol{\tau}|_{m,K} \qquad \forall\, \boldsymbol{\tau} \in \mathbb{H}^m(K) \,. \tag{3.6}$$

We now introduce the interpolation operator $\boldsymbol{\Pi}_k^K : \mathbb{H}^1(K) \to H_k^K$, which is defined for each $\boldsymbol{\tau} \in \mathbb{H}^1(K)$ as the unique $\boldsymbol{\Pi}_k^K(\boldsymbol{\tau})$ in H_k^K such that

$$\begin{aligned} 0 &= \int_e (\boldsymbol{\tau} - \boldsymbol{\Pi}_k^K(\boldsymbol{\tau}))\boldsymbol{\nu} \cdot \mathbf{q} && \forall\, \mathbf{q} \in \boldsymbol{\mathcal{B}}_k(e) \,, \quad \forall \text{ edge } e \in \partial K \,, \\ 0 &= \int_K (\boldsymbol{\tau} - \boldsymbol{\Pi}_k^K(\boldsymbol{\tau})) : \nabla \mathbf{p} && \forall\, \mathbf{p} \in \boldsymbol{\mathcal{B}}_k(K) \setminus \{(1,0)^{\mathbf{t}}, (0,1)^{\mathbf{t}}\} \,, \\ 0 &= \int_K (\boldsymbol{\tau} - \boldsymbol{\Pi}_k^K(\boldsymbol{\tau})) : \boldsymbol{\rho} && \forall\, \boldsymbol{\rho} \in \boldsymbol{\mathcal{G}}_k(K) \,. \end{aligned} \tag{3.7}$$

Concerning the approximation properties of $\boldsymbol{\Pi}_k^K$, we first recall from [5, eq. (3.19)] that for each $\boldsymbol{\tau} \in \mathbb{H}^s(K)$, with $1 \leq s \leq k+1$, there holds

$$\|\boldsymbol{\tau} - \boldsymbol{\Pi}_k^K(\boldsymbol{\tau})\|_{0,K} \;\leq\; C\, h_K^s\, |\boldsymbol{\tau}|_{s,K} \,. \tag{3.8}$$

In addition, for each $\mathbf{p} \in \boldsymbol{\mathcal{B}}_k(K)$ we readily find that

$$\int_K \mathbf{div}(\boldsymbol{\tau} - \boldsymbol{\Pi}_k^K(\boldsymbol{\tau})) \cdot \mathbf{p} \;=\; -\int_K (\boldsymbol{\tau} - \boldsymbol{\Pi}_k^K(\boldsymbol{\tau})) : \nabla \mathbf{p} + \int_{\partial K} (\boldsymbol{\tau} - \boldsymbol{\Pi}_k^K(\boldsymbol{\tau}))\boldsymbol{\nu} \cdot \mathbf{p} \;=\; 0,$$

which, thanks to the fact $\mathbf{div}(\boldsymbol{\Pi}_k^K(\boldsymbol{\tau})) \in \mathbf{P}_k(K)$, implies that

$$\mathbf{div}(\boldsymbol{\Pi}_k^K(\boldsymbol{\tau})) \;=\; \mathcal{P}_k^K(\mathbf{div}(\boldsymbol{\tau})) \qquad \forall\, \boldsymbol{\tau} \in \mathbb{H}^1(K) \,. \tag{3.9}$$

In this way, applying (3.9) and (3.5), we deduce that for each $\boldsymbol{\tau} \in \mathbb{H}^1(K)$, such that $\mathbf{div}(\boldsymbol{\tau}) \in \mathbf{H}^s(K)$, with $0 \leq s \leq k+1$, there holds

$$\|\mathbf{div}(\boldsymbol{\tau}) - \mathbf{div}(\boldsymbol{\Pi}_k^K(\boldsymbol{\tau}))\|_{0,K} \;\leq\; C\, h_K^s\, |\mathbf{div}(\boldsymbol{\tau})|_{s,K} \,, \tag{3.10}$$

which, together with (3.8), allows us to prove the following lemma.

Lemma 3.1. *Let $K \in \mathcal{T}_h$, and let s be an integer such that $1 \leq s \leq k+1$. Then, there exists a constant $C > 0$, independent of K, such that for each $\boldsymbol{\tau} \in \mathbb{H}^s(K)$ such that $\mathbf{div}(\boldsymbol{\tau}) \in \mathbf{H}^s(K)$, there holds*

$$\|\boldsymbol{\tau} - \boldsymbol{\Pi}_k^K(\boldsymbol{\tau})\|_{\mathbf{div};K} \;\leq\; C\, h_K^s \Big\{ |\boldsymbol{\tau}|_{s,K} \,+\, |\mathbf{div}(\boldsymbol{\tau})|_{s,K} \Big\} \,. \tag{3.11}$$

Proof. It follows straightforwardly from (3.8) and (3.10). □

3.3 The discrete scheme

In what follows we define the mixed virtual element scheme itself for our nonlinear problem (2.12). In this regard, we first notice, thanks to (3.3), that the functional $\mathbf{F}$ (cf. (2.14)) is explicitly computable for all $(\mathbf{s},\boldsymbol{\tau}) \in X_k^h \times H_k^h$, whereas for each $K \in \mathcal{T}_h$ the local version $\mathbf{A}^K : (X_k^K \times H_k^K) \to (X_k^K \times H_k^K)'$ of the nonlinear operator $\mathbf{A}$, which is defined for all $(\mathbf{r},\boldsymbol{\zeta}),(\mathbf{s},\boldsymbol{\tau}) \in X_k^K \times H_k^K$ by

$$\begin{aligned}[\mathbf{A}^K(\mathbf{r},\boldsymbol{\zeta}),(\mathbf{s},\boldsymbol{\tau})] \,:=\, \int_K \mu(|\mathbf{r}|)\mathbf{r} : \mathbf{s} \,-\, \int_K \mathbf{s} : \boldsymbol{\zeta}^{\mathbf{d}} \,+\, \int_K \mathbf{r} : \boldsymbol{\tau}^{\mathbf{d}} \\ +\, \kappa \int_K \Big\{ \boldsymbol{\zeta}^{\mathbf{d}} - \mu(|\mathbf{r}|)\mathbf{r} \Big\} : \boldsymbol{\tau}^{\mathbf{d}} \,+\, \frac{1}{\alpha} \int_K \mathbf{div}(\boldsymbol{\zeta}) \cdot \mathbf{div}(\boldsymbol{\tau}) \,,\end{aligned} \tag{3.12}$$

is not computable since $\boldsymbol{\zeta}$ and $\boldsymbol{\tau}$ are not known on the whole $K \in \mathcal{T}_h$. In order to deal with this difficulty, we now recall, as it was remarked in [5, Section 3.2], that the degrees of freedom introduced in (3.4) do allow the explicit calculation of $\boldsymbol{\mathcal{P}}_k^K(\boldsymbol{\tau})$ for each $\boldsymbol{\tau} \in H_k^K$. Indeed, given $\mathbf{p} \in \mathbb{P}_k(K)$, we utilize the decomposition $\mathbb{P}_k(K) = \boldsymbol{\mathcal{G}}_k^{\perp}(K) \oplus \boldsymbol{\mathcal{G}}_k(K)$ to write $\mathbf{p} = \nabla \mathbf{q} + \boldsymbol{\rho}$, with $\mathbf{q} \in \mathbf{P}_{k+1}(K)$ and $\boldsymbol{\rho} \in \boldsymbol{\mathcal{G}}_k(K)$, whence we find that

$$\int_K \boldsymbol{\tau} : \mathbf{p} \;=\; \int_K \boldsymbol{\tau} : \nabla \mathbf{q} + \int_K \boldsymbol{\tau} : \boldsymbol{\rho} \,=\, -\int_K \mathbf{q} \cdot \mathbf{div}(\boldsymbol{\tau}) \,+\, \int_{\partial K} \boldsymbol{\tau}\boldsymbol{\nu} \cdot \mathbf{q} \,+\, \int_K \boldsymbol{\tau} : \boldsymbol{\rho} \,.$$

In this way, it readily follows from (3.3) and (3.4) that the foregoing expression, and hence $\boldsymbol{\mathcal{P}}_k^K(\boldsymbol{\tau})$, are both computable. Then, we now let $\mathbf{A}_h^K : (X_k^K \times H_k^K) \to (X_k^K \times H_k^K)'$ be the computable local discrete nonlinear operator approximating (3.12), which is defined by

$$\begin{aligned}[\mathbf{A}_h^K(\mathbf{r},\boldsymbol{\zeta}),(\mathbf{s},\boldsymbol{\tau})] \,:=\, [\mathbb{A}(\mathbf{r}),\mathbf{s} - \kappa(\boldsymbol{\mathcal{P}}_k^K(\boldsymbol{\tau}))^{\mathbf{d}}] \,-\, \int_\Omega (\boldsymbol{\mathcal{P}}_k^K(\boldsymbol{\zeta}))^{\mathbf{d}} : \mathbf{s} \,+\, \int_\Omega (\boldsymbol{\mathcal{P}}_k^K(\boldsymbol{\tau}))^{\mathbf{d}} : \mathbf{r} \\ +\, \kappa \int_\Omega (\boldsymbol{\mathcal{P}}_k^K(\boldsymbol{\zeta}))^{\mathbf{d}} : (\boldsymbol{\mathcal{P}}_k^K(\boldsymbol{\tau}))^{\mathbf{d}} \,+\, \frac{1}{\alpha} \int_\Omega \mathbf{div}(\boldsymbol{\zeta}) \cdot \mathbf{div}(\boldsymbol{\tau}) \,+\, \mathcal{S}^K(\boldsymbol{\zeta} - \boldsymbol{\mathcal{P}}_k^K(\boldsymbol{\zeta}), \boldsymbol{\tau} - \boldsymbol{\mathcal{P}}_k^K(\boldsymbol{\tau})) \,,\end{aligned} \tag{3.13}$$

for all $(\mathbf{r},\boldsymbol{\zeta}),(\mathbf{s},\boldsymbol{\tau}) \in X_k^K \times H_k^K$, where $\mathcal{S}^K : H_k^K \times H_k^K \to \mathrm{R}$ is any symmetric and positive bilinear form verifying (see [3, Section 4.6] or [5, Section 3.3])

$$\widehat{c}_0 \|\boldsymbol{\zeta}\|_{0,K}^2 \;\leq\; \mathcal{S}^K(\boldsymbol{\zeta},\boldsymbol{\zeta}) \;\leq\; \widehat{c}_1 \|\boldsymbol{\zeta}\|_{0,K}^2 \qquad \forall\, \boldsymbol{\zeta} \in H_k^K, \tag{3.14}$$

with constants $\widehat{c}_0, \widehat{c}_1 > 0$ depending only on $C_{\mathcal{T}}$. In particular, for the numerical results reported below in Section 5 we take $\mathcal{S}^K$ as the bilinear form whose associated matrix with respect to the canonical basis of H_k^K determined by the degrees of freedom (3.4), is the identity matrix. Equivalently, letting n_k^K be the dimension of H_k^K and denoting by $m_{j,K}$, $j \in \{1,2,\ldots,n_k^K\}$, the degrees of freedom given by (3.4), we set

$$\mathcal{S}^K(\boldsymbol{\zeta},\boldsymbol{\tau}) \,:=\, \sum_{j=1}^{n_k^K} m_{j,K}(\boldsymbol{\zeta})\, m_{j,K}(\boldsymbol{\tau}) \qquad \forall\, (\boldsymbol{\zeta},\boldsymbol{\tau}) \,\in\, H_k^K \times H_k^K \,.$$

According to (3.13), we now introduce the global discrete nonlinear operator $\mathbf{A}_h : (X_k^h \times H_k^h) \to (X_k^h \times H_k^h)'$ as

$$[\mathbf{A}_h(\mathbf{r},\boldsymbol{\zeta}),(\mathbf{s},\boldsymbol{\tau})] \,:=\, \sum_{K \in \mathcal{T}_h} [\mathbf{A}_h^K(\mathbf{r},\boldsymbol{\zeta}),(\mathbf{s},\boldsymbol{\tau})] \qquad \forall\, (\mathbf{r},\boldsymbol{\zeta}),(\mathbf{s},\boldsymbol{\tau}) \in X_k^h \times H_k^h. \tag{3.15}$$

Therefore, the mixed virtual element scheme associated with the augmented formulation (2.12) reads: Find $(\mathbf{t}_h,\boldsymbol{\sigma}_h) \in X_k^h \times H_k^h$ such that

$$[\mathbf{A}_h(\mathbf{t}_h,\boldsymbol{\sigma}_h),(\mathbf{s}_h,\boldsymbol{\tau}_h)] \;=\; [\mathbf{F},(\mathbf{s}_h,\boldsymbol{\tau}_h)] \qquad \forall\, (\mathbf{s}_h,\boldsymbol{\tau}_h) \in X_k^h \times H_k^h \,. \tag{3.16}$$

3.4 Analysis of the discrete scheme

In this section we develop the solvability analysis of our mixed virtual element scheme (3.16). First, recalling that the local orthogonal projectors $\mathcal{P}_k^K : \mathbf{L}^2(K) \to \mathbf{P}_k(K)$ and $\boldsymbol{\mathcal{P}}_k^K : \mathbb{L}^2(K) \to \mathbb{P}_k(K)$ were introduced in Section 3.2, we now denote by $\mathcal{P}_k^h$ and $\boldsymbol{\mathcal{P}}_k^h$, respectively, its global counterparts, that is, given $\mathbf{v} \in \mathbf{L}^2(\Omega)$ and $\boldsymbol{\zeta} \in \mathbb{L}^2(\Omega)$, we let

$$\mathcal{P}_k^h(\mathbf{v})\big|_K := \mathcal{P}_k^K(\mathbf{v}\big|_K) \quad \text{and} \quad \boldsymbol{\mathcal{P}}_k^h(\boldsymbol{\zeta})\big|_K := \boldsymbol{\mathcal{P}}_k^K(\boldsymbol{\zeta}\big|_K) \quad \forall\, K \in \mathcal{T}_h.$$

Further, given the local bilinear form $\mathcal{S}^K : H_k^K \times H_k^K \to \mathrm{R}$, we now define the symmetric and positive definite global bilinear form $\mathcal{S}_h : H_k^h \times H_k^h \to \mathrm{R}$ as

$$\mathcal{S}_h(\boldsymbol{\zeta}, \boldsymbol{\tau}) \;:=\; \sum_{K \in \mathcal{T}_h} \mathcal{S}^K(\boldsymbol{\zeta}|_K, \boldsymbol{\tau}|_K) \qquad \forall\, (\boldsymbol{\zeta}, \boldsymbol{\tau}) \in H_k^h,$$

which according to (3.14), satisfies

$$\widehat{c}_0 \|\boldsymbol{\zeta}\|_{0,\Omega}^2 \;\leq\; \mathcal{S}_h(\boldsymbol{\zeta}, \boldsymbol{\zeta}) \;\leq\; \widehat{c}_1 \|\boldsymbol{\zeta}\|_{0,\Omega}^2 \qquad \forall\, \boldsymbol{\zeta} \in H_k^h. \tag{3.17}$$

Now, the Lipschitz-continuity of the discrete nonlinear operator $\mathbf{A}_h$ on $X_k^h \times H_k^h$ (cf. (3.15)) is established in the following lemma.

Lemma 3.2. *There exists a constant $\gamma > 0$, independent of h, such that*

$$\|\mathbf{A}_h(\mathbf{t}, \boldsymbol{\sigma}) - \mathbf{A}_h(\mathbf{r}, \boldsymbol{\zeta})\|_{(X \times H)'} \;\leq\; \gamma \|(\mathbf{t}, \boldsymbol{\sigma}) - (\mathbf{r}, \boldsymbol{\zeta})\|_{X \times H} \qquad \forall\, (\mathbf{t}, \boldsymbol{\sigma}), (\mathbf{r}, \boldsymbol{\zeta}) \in X_k^h \times H_k^h\,. \tag{3.18}$$

Proof. Given $(\mathbf{t}, \boldsymbol{\sigma}), (\mathbf{r}, \boldsymbol{\zeta}), (\mathbf{s}, \boldsymbol{\tau}) \in X_k^h \times H_k^h$, we first observe that

$$\begin{aligned}
[\mathbf{A}_h(\mathbf{t}, \boldsymbol{\sigma}) - \mathbf{A}_h(\mathbf{r}, \boldsymbol{\zeta}), (\mathbf{s}, \boldsymbol{\tau})] \;&=\; [\mathbb{A}(\mathbf{t}) - \mathbb{A}(\mathbf{r}), \mathbf{s} - \kappa(\boldsymbol{\mathcal{P}}_k^h(\boldsymbol{\tau}))^{\mathbf{d}}] - \int_\Omega \mathbf{s} : (\boldsymbol{\mathcal{P}}_k^h(\boldsymbol{\sigma} - \boldsymbol{\zeta}))^{\mathbf{d}} \\
&+ \quad \int_\Omega (\mathbf{t} - \mathbf{r}) : (\boldsymbol{\mathcal{P}}_k^h(\boldsymbol{\tau}))^{\mathbf{d}} \;+\; \kappa \int_\Omega (\boldsymbol{\mathcal{P}}_k^h(\boldsymbol{\sigma} - \boldsymbol{\zeta}))^{\mathbf{d}} : (\boldsymbol{\mathcal{P}}_k^h(\boldsymbol{\tau}))^{\mathbf{d}} \\
&+ \quad \mathcal{S}_h((\boldsymbol{\sigma} - \boldsymbol{\zeta}) - \boldsymbol{\mathcal{P}}_k^h(\boldsymbol{\sigma} - \boldsymbol{\zeta}), \boldsymbol{\tau} - \boldsymbol{\mathcal{P}}_k^h(\boldsymbol{\tau})) \;+\; \frac{1}{\alpha} \int_\Omega \mathbf{div}(\boldsymbol{\sigma} - \boldsymbol{\zeta}) \cdot \mathbf{div}(\boldsymbol{\tau})\,.
\end{aligned}$$

Then, applying the Cauchy-Schwarz inequality, the Lipschitz-continuity of the operator $\mathbb{A}$ (cf. (2.16)), and the upper bound in (3.17), we find that

$$[\mathbf{A}_h(\mathbf{t}, \boldsymbol{\sigma}) - \mathbf{A}_h(\mathbf{r}, \boldsymbol{\zeta}), (\mathbf{s}, \boldsymbol{\tau})] \;\leq\; \gamma \|(\mathbf{t}, \boldsymbol{\sigma}) - (\mathbf{r}, \boldsymbol{\zeta})\|_{X \times H} \|(\mathbf{s}, \boldsymbol{\tau})\|_{X \times H},$$

with γ depending only on γ_0 (cf. (2.2), (2.16)), κ, $\frac{1}{\alpha}$, and $\widehat{c}_1$. In this way, the foregoing equation leads to (3.18), which ends the proof of the lemma. □

The following result provides the discrete analogue of Lemma 2.2.

Lemma 3.3. *Let $\mathbf{A}_h$ be the nonlinear operator defined in* (3.15)*. Assume that the parameter κ satisfy the conditions required by* Lemma 2.2*. Then, there exists a positive constant $\widetilde{C}_{SM}$, independent of h, such that for all $(\mathbf{r}_h, \boldsymbol{\zeta}_h), (\mathbf{s}_h, \boldsymbol{\tau}_h) \in X_k^h \times H_k^h$ there holds*

$$[\mathbf{A}_h(\mathbf{r}_h, \boldsymbol{\zeta}_h) - \mathbf{A}_h(\mathbf{s}_h, \boldsymbol{\tau}_h), (\mathbf{r}_h, \boldsymbol{\zeta}_h) - (\mathbf{s}_h, \boldsymbol{\tau}_h)] \geq \widetilde{C}_{SM} \|(\mathbf{r}_h, \boldsymbol{\zeta}_h) - (\mathbf{s}_h, \boldsymbol{\tau}_h)\|_{X \times H}^2.$$

Proof. Given $(\mathbf{r}_h,\boldsymbol{\zeta}_h),(\mathbf{s}_h,\boldsymbol{\tau}_h)\in X_k^h\times H_k^h$, we have from (3.13) and (3.15) that

$$\begin{aligned}[\mathbf{A}_h(\mathbf{r}_h,\boldsymbol{\zeta}_h)-\mathbf{A}_h(\mathbf{s}_h,\boldsymbol{\tau}_h),(\mathbf{r}_h,\boldsymbol{\zeta}_h)-(\mathbf{s}_h,\boldsymbol{\tau}_h)] \,&=\, [\mathbb{A}(\mathbf{r}_h)-\mathbb{A}(\mathbf{s}_h),\mathbf{r}_h-\mathbf{s}_h]\\ &+\,\kappa\,\|(\boldsymbol{\mathcal{P}}_k^h(\boldsymbol{\zeta}_h-\boldsymbol{\tau}_h))^{\mathbf{d}}\|_{0,\Omega}^2\,-\,\kappa[\mathbb{A}(\mathbf{r}_h)-\mathbb{A}(\mathbf{s}_h),(\boldsymbol{\mathcal{P}}_k^h(\boldsymbol{\zeta}_h-\boldsymbol{\tau}_h))^{\mathbf{d}}]\\ &+\,\frac{1}{\alpha}\|\mathbf{div}(\boldsymbol{\zeta}_h-\boldsymbol{\tau}_h)\|_{0,\Omega}^2\,+\,\mathcal{S}_h((\boldsymbol{\zeta}_h-\boldsymbol{\tau}_h)-\boldsymbol{\mathcal{P}}_k^h(\boldsymbol{\zeta}_h-\boldsymbol{\tau}_h),(\boldsymbol{\zeta}_h-\boldsymbol{\tau}_h)-\boldsymbol{\mathcal{P}}_k^h(\boldsymbol{\zeta}_h-\boldsymbol{\tau}_h))\,.\end{aligned}$$

Then, using the Cauchy-Schwarz and Young inequalities, the Lipschitz-continuity and strong monotonicity properties of the operator $\mathbb{A}$ (cf. (2.16), (2.17)), and the lower bound in (3.17), we get

$$\begin{aligned}[\mathbf{A}_h(\mathbf{r}_h,\boldsymbol{\zeta}_h)-\mathbf{A}_h(\mathbf{s}_h,\boldsymbol{\tau}_h),(\mathbf{r}_h,\boldsymbol{\zeta}_h)-(\mathbf{s}_h,\boldsymbol{\tau}_h)] \,&\geq\, \left(\alpha_0-\frac{\kappa\gamma_0}{2\delta}\right)\|\mathbf{r}_h-\mathbf{s}_h\|_{0,\Omega}^2\\ &+\,\kappa\,\left(1-\frac{\gamma_0\delta}{2}\right)\|\boldsymbol{\mathcal{P}}_k^h((\boldsymbol{\zeta}_h-\boldsymbol{\tau}_h)^{\mathbf{d}})\|_{0,\Omega}^2\,+\,\frac{1}{\alpha}\|\mathbf{div}(\boldsymbol{\zeta}_h-\boldsymbol{\tau}_h)\|_{0,\Omega}^2\\ &+\,\widehat{c}_0\,\|(\boldsymbol{\zeta}_h-\boldsymbol{\tau}_h)^{\mathbf{d}}-(\boldsymbol{\mathcal{P}}_k^h(\boldsymbol{\zeta}_h-\boldsymbol{\tau}_h))^{\mathbf{d}}\|_{0,\Omega}^2 \qquad (3.19)\\ &\geq\,\left(\alpha_0-\frac{\kappa\gamma_0}{2\delta}\right)\|\mathbf{r}_h-\mathbf{s}_h\|_{0,\Omega}^2\,+\,\frac{1}{\alpha}\|\mathbf{div}(\boldsymbol{\zeta}_h-\boldsymbol{\tau}_h)\|_{0,\Omega}^2\\ &+\,\eta\,\left\{2\|(\boldsymbol{\mathcal{P}}_k^h(\boldsymbol{\zeta}_h-\boldsymbol{\tau}_h))^{\mathbf{d}}\|_{0,\Omega}^2\,+\,2\,\|(\boldsymbol{\zeta}_h-\boldsymbol{\tau}_h)^{\mathbf{d}}-(\boldsymbol{\mathcal{P}}_k^h(\boldsymbol{\zeta}_h-\boldsymbol{\tau}_h))^{\mathbf{d}}\|_{0,\Omega}^2\right\}\,,\end{aligned}$$

where $\eta\,:=\,\dfrac{1}{2}\min\left\{\kappa\left(1-\dfrac{\gamma_0\delta}{2}\right),\widehat{c}_0\right\}$. Next, applying the parallelogram law in the last term of the foregoing inequality, we arrive at

$$2\,\|(\boldsymbol{\mathcal{P}}_k^h(\boldsymbol{\zeta}_h-\boldsymbol{\tau}_h))^{\mathbf{d}}\|_{0,\Omega}^2\,+\,2\,\|(\boldsymbol{\zeta}_h-\boldsymbol{\tau}_h)^{\mathbf{d}}-(\boldsymbol{\mathcal{P}}_k^h(\boldsymbol{\zeta}_h-\boldsymbol{\tau}_h))^{\mathbf{d}}\|_{0,\Omega}^2\,\geq\,\|(\boldsymbol{\zeta}_h-\boldsymbol{\tau}_h)^{\mathbf{d}}\|_{0,\Omega}^2\,,$$

which replaced back into (3.19), and using Lemma 2.1, finishes the proof with the constant

$$\widetilde{C}_{SM}:=\min\left\{\left(\alpha_0-\frac{\kappa\gamma_0}{2\delta}\right),\;c(\Omega)\min\left\{\eta,\frac{1}{2\alpha}\right\},\;\frac{1}{2\alpha}\right\}.\qquad\square$$

The unique solvability and stability of the actual Galerkin scheme (3.16) is established now

Theorem 3.1. *Assume that given $\delta\in\left(0,\dfrac{2}{\gamma_0}\right)$, the parameter κ lies in $\left(0,\dfrac{2\delta\alpha_0}{\gamma_0}\right)$. Then, there exists a unique $(\mathbf{t}_h,\boldsymbol{\sigma}_h)\in X_k^h\times H_k^h$ solution of* (3.16)*, and there exists a positive constant C, independent of h, such that*

$$\|(\mathbf{t}_h,\boldsymbol{\sigma}_h)\|_{X\times H}\,\leq\,C\left\{\|\mathbf{f}\|_{0,\Omega}\,+\,\|\mathbf{g}\|_{1/2,\Gamma}\right\}.$$

Proof. Thanks to Lemmas 3.2 and 3.3, the proof is a direct application of [29, Theorem 25.B]. $\square$

4 The a priori error estimates

We now aim to derive the priori error estimates for the continuous and discrete formulations (2.12) and (3.16). For this, given the local interpolation $\boldsymbol{\Pi}_k^K$ introduced in the Section 3.2, we denote by $\boldsymbol{\Pi}_k^h$ its global counterpart, that is, for all $\boldsymbol{\zeta}\in\mathbb{H}(\mathbf{div};\Omega)$ such that $\boldsymbol{\zeta}\big|_K\in\mathbb{H}^1(K)$ for all $K\in\mathcal{T}_h$, we let

$$\boldsymbol{\Pi}_k^h(\boldsymbol{\zeta})\big|_K\,:=\,\boldsymbol{\Pi}_k^K(\boldsymbol{\zeta}\big|_K)\qquad\forall\,K\in\mathcal{T}_h\,.$$

We begin our analysis with the following lemma.

Lemma 4.1. *There exists a constant $c_1 > 0$, depending only on κ and $\widehat{c}_1$ (cf. (3.14)), such that*

$$[\mathbf{A}_h(\mathbf{r}_h,\boldsymbol{\zeta}_h) - \mathbf{A}(\mathbf{r}_h,\boldsymbol{\zeta}_h),(\mathbf{s}_h,\boldsymbol{\tau}_h)] \;\leq\; c_1\,\|\boldsymbol{\zeta}_h - \boldsymbol{\mathcal{P}}_k^h(\boldsymbol{\zeta}_h)\|_{0,\Omega}\,\|(\mathbf{s}_h,\boldsymbol{\tau}_h)\|_{X\times H}$$

for all $(\mathbf{r}_h,\boldsymbol{\zeta}_h),(\mathbf{s}_h,\boldsymbol{\tau}_h) \in X_k^h \times H_k^h$.

Proof. We first observe, according to the definitions of $\mathbf{A}_h$ (cf. (3.13), (3.15)) and $\mathbf{A}$ (cf. (2.13)), that

$$\begin{aligned}
[\mathbf{A}_h(\mathbf{r}_h,\boldsymbol{\zeta}_h) - \mathbf{A}(\mathbf{r}_h,\boldsymbol{\zeta}_h),(\mathbf{s}_h,\boldsymbol{\tau}_h)] \;&=\; \int_\Omega \Big\{\boldsymbol{\zeta}_h^{\mathbf{d}} - (\boldsymbol{\mathcal{P}}_k^h(\boldsymbol{\zeta}_h))^{\mathbf{d}}\Big\} : \mathbf{s}_h + \int_\Omega \Big\{(\boldsymbol{\mathcal{P}}_k^h(\boldsymbol{\tau}_h))^{\mathbf{d}} - \boldsymbol{\tau}_h^{\mathbf{d}}\Big\} : \mathbf{r}_h \\
&+ \kappa \int_\Omega \Big\{\boldsymbol{\tau}_h^{\mathbf{d}} - (\boldsymbol{\mathcal{P}}_k^h(\boldsymbol{\tau}_h))^{\mathbf{d}}\Big\} : \mu(|\mathbf{r}_h|)\,\mathbf{r}_h \;+\; \kappa \int_\Omega (\boldsymbol{\mathcal{P}}_k^h(\boldsymbol{\zeta}_h))^{\mathbf{d}} : (\boldsymbol{\mathcal{P}}_k^h(\boldsymbol{\tau}_h))^{\mathbf{d}} \;-\; \kappa \int_\Omega \boldsymbol{\zeta}_h^{\mathbf{d}} : \boldsymbol{\tau}_h^{\mathbf{d}} \\
&+ \mathcal{S}_h(\boldsymbol{\zeta}_h - \boldsymbol{\mathcal{P}}_k^h(\boldsymbol{\zeta}_h),\boldsymbol{\tau}_h - \boldsymbol{\mathcal{P}}_k^h(\boldsymbol{\tau}_h))\,,
\end{aligned}$$

for all $(\mathbf{r}_h,\boldsymbol{\zeta}_h),(\mathbf{s}_h,\boldsymbol{\tau}_h) \in X_k^h \times H_k^h$. Then, using that $\mathbf{s}_h\big|_K$, $\mathbf{r}_h\big|_K$, and $\mu(|\mathbf{r}_h|)\,\mathbf{r}_h\big|_K$ belong to $\mathbb{P}_k(K)$ for each $K \in \mathcal{T}_h$, we deduce that the first three terms on the right hand side of the foregoing equation vanish, whereas the fourth one reduces to $\kappa \displaystyle\int_\Omega (\boldsymbol{\mathcal{P}}_k^h(\boldsymbol{\zeta}_h))^{\mathbf{d}} : \boldsymbol{\tau}_h^{\mathbf{d}}$, and hence $\mathbf{A}_h$ becomes

$$[\mathbf{A}_h(\mathbf{r}_h,\boldsymbol{\zeta}_h) - \mathbf{A}(\mathbf{r}_h,\boldsymbol{\zeta}_h),(\mathbf{s}_h,\boldsymbol{\tau}_h)] \;=\; \kappa \int_\Omega (\boldsymbol{\mathcal{P}}_k^h(\boldsymbol{\zeta}_h) \;-\; \boldsymbol{\zeta}_h)^{\mathbf{d}} : \boldsymbol{\tau}_h^{\mathbf{d}} \;+\; \mathcal{S}_h(\boldsymbol{\zeta}_h - \boldsymbol{\mathcal{P}}_k^h(\boldsymbol{\zeta}_h),\boldsymbol{\tau}_h - \boldsymbol{\mathcal{P}}_k^h(\boldsymbol{\tau}_h))\,.$$

In this way, using the Cauchy-Schwarz inequality, the symmetry of $\mathcal{S}_h$, and the upper bound in (3.17), we find that

$$\begin{aligned}
[\mathbf{A}_h(\mathbf{r}_h,\boldsymbol{\zeta}_h) - \mathbf{A}(\mathbf{r}_h,\boldsymbol{\zeta}_h),(\mathbf{s}_h,\boldsymbol{\tau}_h)] \;&\leq\; \kappa\,\|\boldsymbol{\zeta}_h - \boldsymbol{\mathcal{P}}_k^h(\boldsymbol{\zeta}_h)\|_{0,\Omega}\|\boldsymbol{\tau}_h\|_{0,\Omega} \\
&+\; \Big\{\mathcal{S}_h(\boldsymbol{\zeta}_h - \boldsymbol{\mathcal{P}}_k^h(\boldsymbol{\zeta}_h),\boldsymbol{\zeta}_h - \boldsymbol{\mathcal{P}}_k^h(\boldsymbol{\zeta}_h))\Big\}^{1/2}\Big\{\mathcal{S}_h(\boldsymbol{\tau}_h - \boldsymbol{\mathcal{P}}_k^h(\boldsymbol{\tau}_h),\boldsymbol{\tau}_h - \boldsymbol{\mathcal{P}}_k^h(\boldsymbol{\tau}_h))\Big\}^{1/2} \\
&\leq\; c_1\,\|\boldsymbol{\zeta}_h - \boldsymbol{\mathcal{P}}_k^h(\boldsymbol{\zeta}_h)\|_{0,\Omega}\|(\mathbf{s}_h,\boldsymbol{\tau}_h)\|_{X\times H}\,,
\end{aligned}$$

with $c_1 := 2\,\max\{\kappa,\widehat{c}_1\}$, which completes the proof. □

Then, we have the following main result.

Theorem 4.1. *Let $(\mathbf{t},\boldsymbol{\sigma}) \in X \times H$ and $(\mathbf{t}_h,\boldsymbol{\sigma}_h) \in X_k^h \times H_k^h$ be the unique solutions of the continuous and discrete schemes (2.12) and (3.16), respectively, and assume that $\boldsymbol{\sigma}\big|_K \in \mathbb{H}^1(K)$ for all $K \in \mathcal{T}_h$. Then, there exists a positive constant $C > 0$, independent of h, such that*

$$\|\mathbf{t} - \mathbf{t}_h\|_{0,\Omega} + \|\boldsymbol{\sigma} - \boldsymbol{\sigma}_h\|_{\mathbf{div};\Omega} \leq C\,\Big\{\|\mathbf{t} - \boldsymbol{\mathcal{P}}_k^h(\mathbf{t})\|_{0,\Omega} + \|\boldsymbol{\sigma} - \boldsymbol{\Pi}_k^h(\boldsymbol{\sigma})\|_{\mathbf{div},\Omega} + \|\boldsymbol{\sigma} - \boldsymbol{\mathcal{P}}_k^h(\boldsymbol{\sigma})\|_{0,\Omega}\Big\}\,. \quad (4.1)$$

Proof. We begin by observing, due to the triangle inequality, that

$$\|\mathbf{t} - \mathbf{t}_h\|_{0,\Omega} + \|\boldsymbol{\sigma} - \boldsymbol{\sigma}_h\|_{\mathbf{div};\Omega} \;\leq\; \|\mathbf{t} - \boldsymbol{\mathcal{P}}_k^h(\mathbf{t})\|_{0,\Omega} + \|\boldsymbol{\sigma} - \boldsymbol{\Pi}_k^h(\boldsymbol{\sigma})\|_{\mathbf{div};\Omega} + \|\delta_h^{\mathbf{t}}\|_{0,\Omega} + \|\delta_h^{\boldsymbol{\sigma}}\|_{\mathbf{div};\Omega}, \quad (4.2)$$

where $(\delta_h^{\mathbf{t}},\delta_h^{\boldsymbol{\sigma}}) := (\boldsymbol{\mathcal{P}}_k^h(\mathbf{t}) - \mathbf{t}_h, \boldsymbol{\Pi}_k^h(\boldsymbol{\sigma}) - \boldsymbol{\sigma}_h) \in X_k^h \times H_k^h$. Then, applying the strong monotonicity of $\mathbf{A}_h$ (cf. Lemma 3.3) with $(\mathbf{r}_h,\boldsymbol{\zeta}_h) := (\boldsymbol{\mathcal{P}}_k^h(\mathbf{t}),\boldsymbol{\Pi}_k^h(\boldsymbol{\sigma}))$ and $(\mathbf{s}_h,\boldsymbol{\tau}_h) := (\mathbf{t}_h,\boldsymbol{\sigma}_h)$, and the equations (3.16) and (2.12), we obtain that

$$\begin{aligned}
\widetilde{C}_{SM}\|(\delta_h^{\mathbf{t}},\delta_h^{\boldsymbol{\sigma}})\|_{X\times H}^2 \;&\leq\; [\mathbf{A}_h(\boldsymbol{\mathcal{P}}_k^h(\mathbf{t}),\boldsymbol{\Pi}_k^h(\boldsymbol{\sigma})) - \mathbf{A}_h(\mathbf{t}_h,\boldsymbol{\sigma}_h),(\delta_h^{\mathbf{t}},\delta_h^{\boldsymbol{\sigma}})] \\
&=\; [\mathbf{A}_h(\boldsymbol{\mathcal{P}}_k^h(\mathbf{t}),\boldsymbol{\Pi}_k^h(\boldsymbol{\sigma})),(\delta_h^{\mathbf{t}},\delta_h^{\boldsymbol{\sigma}})] - [\mathbf{A}_h(\mathbf{t}_h,\boldsymbol{\sigma}_h),(\delta_h^{\mathbf{t}},\delta_h^{\boldsymbol{\sigma}})] \\
&=\; [\mathbf{A}_h(\boldsymbol{\mathcal{P}}_k^h(\mathbf{t}),\boldsymbol{\Pi}_k^h(\boldsymbol{\sigma})),(\delta_h^{\mathbf{t}},\delta_h^{\boldsymbol{\sigma}})] - [\mathbf{A}(\mathbf{t},\boldsymbol{\sigma}),(\delta_h^{\mathbf{t}},\delta_h^{\boldsymbol{\sigma}})]\,,
\end{aligned}$$

from which, adding and subtracting $[\mathbf{A}(\boldsymbol{\mathcal{P}}_k^h(\mathbf{t}),\boldsymbol{\Pi}_k^h(\boldsymbol{\sigma})),(\delta_h^{\mathbf{t}},\delta_h^{\boldsymbol{\sigma}})]$, we obtain

$$\begin{aligned}\widetilde{C}_{SM}\|(\delta_h^{\mathbf{t}},\delta_h^{\boldsymbol{\sigma}})\|_{X\times H}^2 \,\leq\, &[\mathbf{A}_h(\boldsymbol{\mathcal{P}}_k^h(\mathbf{t}),\boldsymbol{\Pi}_k^h(\boldsymbol{\sigma}))-\mathbf{A}(\boldsymbol{\mathcal{P}}_k^h(\mathbf{t}),\boldsymbol{\Pi}_k^h(\boldsymbol{\sigma})),(\delta_h^{\mathbf{t}},\delta_h^{\boldsymbol{\sigma}})]\\ &+\,[\mathbf{A}(\boldsymbol{\mathcal{P}}_k^h(\mathbf{t}),\boldsymbol{\Pi}_k^h(\boldsymbol{\sigma}))-\mathbf{A}(\mathbf{t},\boldsymbol{\sigma}),(\delta_h^{\mathbf{t}},\delta_h^{\boldsymbol{\sigma}})]\,.\end{aligned}\tag{4.3}$$

The two expressions on the right-hand side of (4.3) are bounded in what follows. Indeed, applying Lemma 4.1, and then adding and subtracting $\boldsymbol{\sigma}-\boldsymbol{\mathcal{P}}_k^h(\boldsymbol{\sigma})$, we find that

$$\begin{aligned}[\mathbf{A}_h(\boldsymbol{\mathcal{P}}_k^h(\mathbf{t}),\boldsymbol{\Pi}_k^h(\boldsymbol{\sigma}))-\mathbf{A}(\boldsymbol{\mathcal{P}}_k^h(\mathbf{t}),\boldsymbol{\Pi}_k^h(\boldsymbol{\sigma})),(\delta_h^{\mathbf{t}},\delta_h^{\boldsymbol{\sigma}})] \,&\leq\, c_1\,\|\boldsymbol{\Pi}_k^h(\boldsymbol{\sigma})-\boldsymbol{\mathcal{P}}_k^h\{\boldsymbol{\Pi}_k^h(\boldsymbol{\sigma})\}\|_{0,\Omega}\,\|(\delta_h^{\mathbf{t}},\delta_h^{\boldsymbol{\sigma}})\|_{X\times H}\\ &\leq\, c_1\Big\{\|\boldsymbol{\sigma}-\boldsymbol{\Pi}_k^h(\boldsymbol{\sigma})\|_{\mathbf{div};\Omega}\,+\,\|\boldsymbol{\sigma}-\boldsymbol{\mathcal{P}}_k^h(\boldsymbol{\sigma})\|_{0,\Omega}\,+\,\|\boldsymbol{\mathcal{P}}_k^h\{\boldsymbol{\sigma}-\boldsymbol{\Pi}_k^h(\boldsymbol{\sigma})\}\|_{0,\Omega}\Big\}\,\|(\delta_h^{\mathbf{t}},\delta_h^{\boldsymbol{\sigma}})\|_{X\times H}\\ &\leq\, 2\,c_1\Big\{\|\boldsymbol{\sigma}-\boldsymbol{\Pi}_k^h(\boldsymbol{\sigma})\|_{\mathbf{div},\Omega}\,+\,\|\boldsymbol{\sigma}-\boldsymbol{\mathcal{P}}_k^h(\boldsymbol{\sigma})\|_{0,\Omega}\Big\}\,\|(\delta_h^{\mathbf{t}},\delta_h^{\boldsymbol{\sigma}})\|_{X\times H}\,,\end{aligned}\tag{4.4}$$

whereas the Lipschitz-continuity of $\mathbf{A}$ (cf. (2.18)) yields

$$\begin{aligned}&[\mathbf{A}(\mathcal{P}_k^h(\mathbf{t}),\boldsymbol{\Pi}_k^h(\boldsymbol{\sigma}))-\mathbf{A}(\mathbf{t},\boldsymbol{\sigma}),(\delta_h^{\mathbf{t}},\delta_h^{\boldsymbol{\sigma}})]\\ &\qquad\leq\,\sqrt{2}\,L_{\mathbf{A}}\,\Big\{\|\mathbf{t}-\boldsymbol{\mathcal{P}}_k^h(\mathbf{t})\|_{0,\Omega}\,+\,\|\boldsymbol{\sigma}-\boldsymbol{\Pi}_k^h(\boldsymbol{\sigma})\|_{\mathbf{div},\Omega}\Big\}\,\|(\delta_h^{\mathbf{t}},\delta_h^{\boldsymbol{\sigma}})\|_{X\times H}\,.\end{aligned}\tag{4.5}$$

In this way, (4.3), (4.4), and (4.5) yield the existence of $C:=C(\widetilde{C}_{SM},c_1,L_{\mathbf{A}})>0$, such that

$$\|\delta_h^{\mathbf{t}}\|_{0,\Omega}+\|\delta_h^{\boldsymbol{\sigma}}\|_{\mathbf{div};\Omega}\,\leq\,C\,\Big\{\|\mathbf{t}-\boldsymbol{\mathcal{P}}_k^h(\mathbf{t})\|_{0,\Omega}\,+\,\|\boldsymbol{\sigma}-\boldsymbol{\Pi}_k^h(\boldsymbol{\sigma})\|_{\mathbf{div},\Omega}\,+\,\|\boldsymbol{\sigma}-\boldsymbol{\mathcal{P}}_k^h(\boldsymbol{\sigma})\|_{0,\Omega}\Big\}\,,$$

which, together with (4.2), gives (4.1) and ends the proof of the theorem. □

Having established the a priori error estimates for our unknowns, we now provide the corresponding rate of convergence.

Theorem 4.2. *Let $(\mathbf{t},\boldsymbol{\sigma})\in X\times H$ and $(\mathbf{t}_h,\boldsymbol{\sigma}_h)\in X_k^h\times H_k^h$ be the unique solutions of the continuous and discrete schemes* (2.12) *and* (3.16)*, respectively. Assume that for some $s\in[1,k+1]$ there hold $\mathbf{t}\big|_K$, $\boldsymbol{\sigma}\big|_K\in\mathbb{H}^s(K)$, and $\mathbf{div}(\boldsymbol{\sigma})\big|_K\in\mathbf{H}^s(K)$ for each $K\in\mathcal{T}_h$. Then, there exists $C>0$, independent of h, such that*

$$\|\mathbf{t}-\mathbf{t}_h\|_{0,\Omega}\,+\,\|\boldsymbol{\sigma}-\boldsymbol{\sigma}_h\|_{\mathbf{div};\Omega}\,\leq\,C\,h^s\sum_{K\in\mathcal{T}_h}\Big\{|\mathbf{t}|_{s,K}+|\boldsymbol{\sigma}|_{s,K}+|\mathbf{div}(\boldsymbol{\sigma})|_{s,K}\Big\}\,.\tag{4.6}$$

Proof. It follows from (4.1) and a straightforward application of the approximation properties provided by (3.6) and (3.11). □

4.1 Computable approximations of $\boldsymbol{\sigma}, p$ and $\mathbf{u}$

We now introduce the fully computable approximation of $\boldsymbol{\sigma}_h$ given by

$$\widehat{\boldsymbol{\sigma}}_h:=\boldsymbol{\mathcal{P}}_k^h(\boldsymbol{\sigma}_h),\tag{4.7}$$

and establishes next the corresponding a priori error estimate in the $\mathbb{L}^2(\Omega)$-norm, which yields exactly the same rate of convergence given by Theorem 4.2.

Lemma 4.2. *There exists a positive constant C, independent of h, such that*

$$\|\boldsymbol{\sigma}-\widehat{\boldsymbol{\sigma}}_h\|_{0,\Omega}\leq C\,\Big\{\|\mathbf{t}-\boldsymbol{\mathcal{P}}_k^h(\mathbf{t})\|_{0,\Omega}+\|\boldsymbol{\sigma}-\boldsymbol{\Pi}_k^h(\boldsymbol{\sigma})\|_{\mathbf{div},\Omega}+\|\boldsymbol{\sigma}-\boldsymbol{\mathcal{P}}_k^h(\boldsymbol{\sigma})\|_{0,\Omega}\Big\}\,.\tag{4.8}$$

Proof. The proof is similar to [12, Lemma 5.2]. □

Next, as suggested by (2.6) and (2.10), and proceeding as in [12, Section 5.2], we define

$$p_h := -\frac{1}{2}\mathrm{tr}(\widehat{\boldsymbol{\sigma}}_h) \quad \text{and} \quad \mathbf{u}_h := \frac{1}{\alpha}\left\{\mathcal{P}_k^h(\mathbf{f}) + \mathbf{div}(\boldsymbol{\sigma}_h)\right\}, \tag{4.9}$$

which constitute fully computable approximations of the pressure and velocity, respectively. Then, we notice from (2.6) and the first equation of (4.9) that there holds

$$\|p - p_h\|_{0,\Omega} \;=\; \frac{1}{2}\|\mathrm{tr}(\boldsymbol{\sigma} - \widehat{\boldsymbol{\sigma}}_h)\|_{0,\Omega} \;\leq\; \frac{1}{\sqrt{2}}\|\boldsymbol{\sigma} - \widehat{\boldsymbol{\sigma}}_h\|_{0,\Omega},$$

which, together with (4.8), gives the a priori error estimate for the pressure, that is

$$\|p - p_h\|_{0,\Omega} \leq C\left\{\|\mathbf{t} - \boldsymbol{\mathcal{P}}_k^h(\mathbf{t})\|_{0,\Omega} + \|\boldsymbol{\sigma} - \boldsymbol{\Pi}_k^h(\boldsymbol{\sigma})\|_{\mathbf{div},\Omega} + \|\boldsymbol{\sigma} - \boldsymbol{\mathcal{P}}_k^h(\boldsymbol{\sigma})\|_{0,\Omega}\right\}. \tag{4.10}$$

In turn, starting from (2.10) and the second equation of (4.9), and then using again from (2.10) that $\mathbf{f} = \alpha\mathbf{u} - \mathbf{div}(\boldsymbol{\sigma})$, we arrive at

$$\|\mathbf{u} - \mathbf{u}_h\|_{0,\Omega} \leq C\left\{\|\mathbf{u} - \mathcal{P}_k^h(\mathbf{u})\|_{0,\Omega} + \|\mathbf{div}(\boldsymbol{\sigma}) - \mathcal{P}_k^h(\mathbf{div}(\boldsymbol{\sigma}))\|_{0,\Omega} + \|\mathbf{div}(\boldsymbol{\sigma} - \boldsymbol{\sigma}_h)\|_{0,\Omega}\right\},$$

from which, bounding $\|\mathbf{div}(\boldsymbol{\sigma} - \boldsymbol{\sigma}_h)\|_{0,\Omega}$ by $\|(\mathbf{t},\boldsymbol{\sigma}) - (\mathbf{t}_h,\boldsymbol{\sigma}_h)\|_{X\times H}$, and employing the a priori error estimate (4.1) (cf. Theorem 4.1), we conclude that

$$\begin{aligned}\|\mathbf{u} - \mathbf{u}_h\|_{0,\Omega} \;\leq\; C\Big\{&\|\mathbf{u} - \mathcal{P}_k^h(\mathbf{u})\|_{0,\Omega} \;+\; \|\mathbf{div}(\boldsymbol{\sigma}) - \mathcal{P}_k^h(\mathbf{div}(\boldsymbol{\sigma}))\|_{0,\Omega} \\ &+\; \|\mathbf{t} - \boldsymbol{\mathcal{P}}_k^h(\mathbf{t})\|_{0,\Omega} \;+\; \|\boldsymbol{\sigma} - \boldsymbol{\Pi}_k^h(\boldsymbol{\sigma})\|_{\mathbf{div},\Omega} \;+\; \|\boldsymbol{\sigma} - \boldsymbol{\mathcal{P}}_k^h(\boldsymbol{\sigma})\|_{0,\Omega}\Big\}.\end{aligned} \tag{4.11}$$

In this way, we are now able to provide the theoretical rates of convergence for $\widehat{\boldsymbol{\sigma}}_h$, p_h, and $\mathbf{u}_h$.

Theorem 4.3. *Let $(\mathbf{t},\boldsymbol{\sigma}) \in X \times H$ and $(\mathbf{t}_h,\boldsymbol{\sigma}_h) \in X_k^h \times H_k^h$ be the unique solutions of the continuous and discrete schemes* (2.12) *and* (3.16)*, respectively. In addition, let $\widehat{\boldsymbol{\sigma}}_h$ and $(p_h,\mathbf{u}_h)$ be the discrete approximations introduced in* (4.7) *and* (4.9)*, respectively. Assume that for some $s \in [1, k+1]$ there hold $\mathbf{t}\big|_K$, $\boldsymbol{\sigma}\big|_K \in \mathbb{H}^s(K)$, $\mathbf{div}(\boldsymbol{\sigma})\big|_K \in \mathbf{H}^s(K)$, and $\mathbf{u}\big|_K \in \mathbf{H}^s(K)$ for each $K \in \mathcal{T}_h$. Then, there exist positive constants C_1 and C_2, independent of h, such that*

$$\|\boldsymbol{\sigma} - \widehat{\boldsymbol{\sigma}}_h\|_{0,\Omega} + \|p - p_h\|_{0,\Omega} \;\leq\; C_1\, h^s \sum_{K\in\mathcal{T}_h}\left\{|\mathbf{t}|_{s,K} + |\boldsymbol{\sigma}|_{s,K} + |\mathbf{div}(\boldsymbol{\sigma})|_{s,K}\right\}, \tag{4.12}$$

and

$$\|\mathbf{u} - \mathbf{u}_h\|_{0,\Omega} \;\leq\; C_2\, h^s \;, \sum_{K\in\mathcal{T}_h}\left\{|\mathbf{u}|_{s,K} + |\mathbf{t}|_{s,K} + |\boldsymbol{\sigma}|_{s,K} + |\mathbf{div}(\boldsymbol{\sigma})|_{s,K}\right\}. \tag{4.13}$$

Proof. It follows from (4.8), (4.10), (4.11), and a straightforward application of the approximation properties provided by (3.5), (3.6) and (3.11). □

4.2 A convergent approximation of $\boldsymbol{\sigma}$ in the broken $\mathbb{H}(\mathbf{div})$-norm

In this section we proceed as in [12, Section 5.3] and construct a second approximation, denoted by $\boldsymbol{\sigma}_h^\star$, for the pseudostress variable $\boldsymbol{\sigma}$, which has an optimal rate of convergence in the broken $\mathbb{H}(\mathbf{div})$-norm.

To this end, for each $K \in \mathcal{T}_h$ we let $(\cdot,\cdot)_{\mathbf{div};K}$ be the usual $\mathbb{H}(\mathbf{div};K)$-inner product with induced norm $\|\cdot\|_{\mathbf{div};K}$, and let $\boldsymbol{\sigma}_h^\star\big|_K := \boldsymbol{\sigma}_{h,K}^\star \in \mathbb{P}_{k+1}(K)$ be the unique solution of the local problem

$$(\boldsymbol{\sigma}_{h,K}^\star, \boldsymbol{\tau}_h)_{\mathbf{div};K} = \int_K \widehat{\boldsymbol{\sigma}}_h : \boldsymbol{\tau}_h \; + \; \int_K \mathbf{div}(\boldsymbol{\sigma}_h)\cdot \mathbf{div}(\boldsymbol{\tau}_h) \qquad \forall\, \boldsymbol{\tau}_h \in \mathbb{P}_{k+1}(K). \tag{4.14}$$

We stress that $\boldsymbol{\sigma}_{h,K}^\star$ can be explicitly computed for each $K \in \mathcal{T}_h$, independently. Then, the rate of convergence for the broken $\mathbb{H}(\mathbf{div};\Omega)$-norm of $\boldsymbol{\sigma} - \boldsymbol{\sigma}_h^\star$ is established as follows.

Theorem 4.4. *Assume that the hypotheses of Theorem* 4.2 *are satisfied. Then, there exists a positive constant C, independent of h, such that*

$$\left\{ \sum_{K\in\mathcal{T}_h} \|\boldsymbol{\sigma} - \boldsymbol{\sigma}_{h,K}^\star\|^2_{\mathbf{div};K} \right\}^{1/2} \leq C\, h^s \sum_{K\in\mathcal{T}_h} \Big\{ |\mathbf{t}|_{s,K} + |\boldsymbol{\sigma}|_{s,K} + |\mathbf{div}(\boldsymbol{\sigma})|_{s,K} \Big\}. \tag{4.15}$$

Proof. From [12, Lemma 5.3] and the first part in the proof of [12, Theorem 5.5], we find that there exists $C > 0$, independent of h, such that for each $K \in \mathcal{T}_h$ there holds

$$\begin{aligned} \|\boldsymbol{\sigma} - \boldsymbol{\sigma}_{h,K}^\star\|_{\mathbf{div};K} \leq C \Big\{ &\|\boldsymbol{\sigma} - \widehat{\boldsymbol{\sigma}}_h\|_{0,K} \; + \; \|\mathbf{div}(\boldsymbol{\sigma} - \boldsymbol{\sigma}_h)\|_{0,K} \\ &+ \|\boldsymbol{\sigma} - \boldsymbol{\mathcal{P}}_{k+1}^K(\boldsymbol{\sigma})\|_{0,K} \; + \; |\boldsymbol{\sigma} - \boldsymbol{\mathcal{P}}_{k+1}^K(\boldsymbol{\sigma})|_{1,K} \Big\}, \end{aligned}$$

which, after bounding $\|\mathbf{div}(\boldsymbol{\sigma} - \boldsymbol{\sigma}_h)\|_{0,K}$ by $\|\boldsymbol{\sigma} - \boldsymbol{\sigma}_h)\|_{\mathbf{div},K}$, becomes

$$\begin{aligned} \|\boldsymbol{\sigma} - \boldsymbol{\sigma}_{h,K}^\star\|_{\mathbf{div};K} \leq C \Big\{ &\|\boldsymbol{\sigma} - \widehat{\boldsymbol{\sigma}}_h\|_{0,K} \; + \; \|\boldsymbol{\sigma} - \boldsymbol{\sigma}_h\|_{\mathbf{div},K} \\ &+ \|\boldsymbol{\sigma} - \boldsymbol{\mathcal{P}}_{k+1}^K(\boldsymbol{\sigma})\|_{0,K} \; + \; |\boldsymbol{\sigma} - \boldsymbol{\mathcal{P}}_{k+1}^K(\boldsymbol{\sigma})|_{1,K} \Big\}. \end{aligned}$$

Next, summing up the squares of the foregoing equation over all $K \in \mathcal{T}_h$, and employing the estimates (4.6) and (4.12), and the approximation properties of $\boldsymbol{\mathcal{P}}_{k+1}^K$ (cf. [10, Lemma 3.4]), we conclude (4.15), thus ending the proof. □

5 Numerical results

In this section we present three numerical experiments illustrating the performance of the augmented mixed virtual element scheme (3.16) introduced and analized in Sections 3.3 and 3.4, respectively. More precisely, in all the computations we consider the specific virtual element subspaces X_k^h and H_k^h (cf. (3.1)-(3.2)) and associated discrete nonlinear operator $\mathbf{A}_h$ (cf. (3.15)) determined by the definitions of the local subspaces X_k^K and H_k^K, and the $\mathbb{L}^2$-orthogonal projector $\boldsymbol{\mathcal{P}}_k^K$, respectively, with $k \in \{0,1,2\}$. Here we recall, as already remarked in [11, Section 4.1], that the projector introduced in [10, Section 4] is applicable only when the viscosity μ is constant. In fact, this approach was utilized in [12] for the linear Brinkman problem. Now, as in [12, Section 6], the zero mean condition for tensors in the space H_k^h is imposed via a real Lagrange multiplier, which means that, instead of (3.16), we solve the following modified discrete scheme: Find $((\mathbf{t}_h,\boldsymbol{\sigma}_h),\lambda_h) \in (X_k^h \times H_k^h) \times \mathrm{R}$ such that

$$\begin{aligned} [\mathbf{A}_h(\mathbf{t}_h,\boldsymbol{\sigma}_h),(\mathbf{s}_h,\boldsymbol{\tau}_h)] + \lambda_h \int_\Omega \mathrm{tr}(\boldsymbol{\tau}_h) &= [\mathbf{F},(\mathbf{s}_h,\boldsymbol{\tau}_h)] \qquad \forall\, (\mathbf{s}_h,\boldsymbol{\tau}_h) \in X_k^h \times H_k^h, \\ \beta_h \int_\Omega \mathrm{tr}(\boldsymbol{\sigma}_h) &= 0 \qquad\qquad\qquad\quad \forall\, \beta_h \in \mathrm{R}, \end{aligned} \tag{5.1}$$

where λ_h is an artificial unknown introduced just to keep the symmetry of (3.16). Concerning the decompositions of Ω employed in our computations, we consider quasi-uniform triangles, distorted squares, and distorted hexagons.

We begin by introducing additional notations. In what follows, N stands for the total number of degrees of freedom (unknowns) of (5.1), that is

$$N := 2(k+1) \times \{\text{number of edges } e \in \mathcal{T}_h\} + \frac{(k+2)(7k+3)}{2} \times \{\text{number of elements } K \in \mathcal{T}_h\} + 1.$$

Also, the individual errors are defined by

$$\mathbf{e}(\mathbf{t}) := \|\mathbf{t} - \mathbf{t}_h\|_{0,\Omega}, \quad \mathbf{e}_0(\boldsymbol{\sigma}) := \|\boldsymbol{\sigma} - \widehat{\boldsymbol{\sigma}}_h\|_{0,\Omega}, \quad \mathbf{e}(\mathbf{u}) := \|\mathbf{u} - \mathbf{u}_h\|_{0,\Omega}, \quad \mathbf{e}(p) := \|p - \widehat{p}_h\|_{0,\Omega},$$

$$\mathbf{e}_{\mathrm{div}}(\boldsymbol{\sigma}) := \left\{ \sum_{K \in \mathcal{T}_h} \|\boldsymbol{\sigma} - \widehat{\boldsymbol{\sigma}}_h\|^2_{\mathbf{div};K} \right\}^{1/2} \quad \text{and} \quad \mathbf{e}(\boldsymbol{\sigma}^*) := \left\{ \sum_{K \in \mathcal{T}_h} \|\boldsymbol{\sigma} - \boldsymbol{\sigma}^*_h\|^2_{\mathbf{div};K} \right\}^{1/2},$$

where $\widehat{\boldsymbol{\sigma}}_h, \boldsymbol{\sigma}^*_h$ and $(\widehat{p}_h, \mathbf{u}_h)$ are computed according to (4.7), (4.14), and (4.9), respectively, whereas the associated experimental rates of convergence are given by

$$\mathbf{r}(\cdot) := \frac{\log(\mathbf{e}(\cdot)/\mathbf{e}'(\cdot))}{\log(h/h')},$$

where $\mathbf{e}$ and $\mathbf{e}'$ denote the corresponding errors for two consecutive meshes with sizes h and h', respectively. In turn, the nonlinear algebraic systems arising from (5.1) are solved by the Newton method with a tolerance of 10^{-6} and taking as initial iteration the solution of the linear Brinkman problem with $\mu = 1$ (three iterations were required to achieve the given tolerance in each example). The numerical results presented below were obtained using a MATLAB code, in which all the resulting linear systems are solved by the usual instruction "\".

In Example 1 we take the unit square $\Omega := (0,1)^2$, set $\alpha = 1$, and consider the nonlinear viscosity μ given by the Carreau law (2.4) with $\rho_0 = 2$, $\rho_1 = 1$, and $\beta = 5/3$, that is

$$\mu(s) \ := \ 2 \ + \ (1+s^2)^{-1/6} \quad \forall \, s \geq 0 \, .$$

In addition, we choose the data $\mathbf{f}$ and $\mathbf{g}$ so that the exact solution is given by

$$\mathbf{u}(\mathbf{x}) = \begin{pmatrix} -\cos(\pi x_1)\sin(\pi x_2) \\ \\ \sin(\pi x_1)\cos(\pi x_2) \end{pmatrix} \quad \text{and} \quad p(\mathbf{x}) = x_1^2 - x_2^2$$

for all $\mathbf{x} := (x_1, x_2)^{\mathbf{t}} \in \Omega$.

In Example 2 we consider again $\Omega := (0,1)^2$, $\alpha = 1$, and the nonlinear viscosity given by (2.4), but now with $\rho_0 = \rho_1 = 1/2$, and $\beta = 3/2$, that is

$$\mu(s) \ := \ \frac{1}{2} + \frac{1}{2}(1+s^2)^{-1/4} \quad \forall \, s \geq 0 \, .$$

In this case, the data $\mathbf{f}$ and $\mathbf{g}$ are chosen so that the exact solution is given by

$$\mathbf{u}(\mathbf{x}) \ = \ \begin{pmatrix} x_1^2(x_2+1)\exp(-x_1)\left((x_2+1)\cos(x_2+1) + 2\sin(x_2+1)\right) \\ \\ x_1(x_1-2)(x_2+1)^2\exp(-x_1)\sin(x_2+1) \end{pmatrix},$$

and

$$p(\mathbf{x}) \ = \ \sin(2\pi x_1)\sin(2\pi x_2)$$

for all $\mathbf{x} := (x_1, x_2)^{\mathbf{t}} \in \Omega$.

In Example 3 we take the L-shaped domain $\Omega := (-1,1)^2 \setminus [0,1]^2$, set again $\alpha = 1$, and consider the same nonlinearity μ from Example 2. Then, we choose the data $\mathbf{f}$ and $\mathbf{g}$ so that the exact solution is given by

$$\mathbf{u}(\mathbf{x}) \;=\; \begin{pmatrix} (1 + x_1 - \exp(x_1))(1 - \cos(x_2)) \\ \\ (1 - \exp(x_1))(\sin(x_2) - x_2) \end{pmatrix} \quad \text{and} \quad p(\mathbf{x}) \;=\; (x_1^2 + x_2^2)^{1/3} - p_0$$

for all $\mathbf{x} := (x_1, x_2)^{\mathbf{t}} \in \Omega$, where $p_0 \in \mathrm{R}$ is such that $\int_\Omega p = 0$. Note in this example that the partial derivatives of p, and hence, in particular $\mathbf{div}(\boldsymbol{\sigma})$, are singular at the origin. More precisely, because of the power $1/3$, there holds $\boldsymbol{\sigma} \in \mathbb{H}^{5/3-\epsilon}(\Omega)$ and $\mathbf{div}(\boldsymbol{\sigma}) \in \mathbf{H}^{2/3-\epsilon}(\Omega)$ for each $\epsilon > 0$.

Finally, we remark that for all three examples the explicit constants γ_0 and α_0 are defined according to (2.5), and that the stabilization parameter κ is taken as 0.4, which is easily shown to satisfy the assumption required in Lemma 3.3.

In Tables 5.1 up to 5.6 we summarize the convergence history of the augmented mixed virtual element scheme (5.1) as applied to Example 1 and 2. We notice there that the rate of convergence $O(h^{k+1})$ predicted by Theorems 4.3 and 4.4 (when $s = k+1$) is achieved by all the unknowns for these smooth examples, for triangular as well as for quadrilateral and hexagonal meshes. In particular, these results confirm that our postprocessed stress $\boldsymbol{\sigma}_h^*$ improves in one power the non-satisfactory order provided by the first approximation $\widehat{\boldsymbol{\sigma}}_h$ with respect to the broken $\mathbb{H}(\mathbf{div})$-norm. Next, in Tables 5.7 up to 5.9 we display the corresponding convergence history of Example 3. As predicted by the theory, and due to the limited regularity of p and $\boldsymbol{\sigma}$ in this case, we observe that the orders $O(h^{\min\{k+1,5/3\}})$ and $O(h^{2/3})$ are attained by $(\boldsymbol{\sigma}_h, p_h)$ and $\boldsymbol{\sigma}_h^*$, respectively. In addition, we observe that $\mathbf{u}_h$ shows a convergence rate of $O(h^{\min\{k,5/3\}+1})$. This behaviour of the error $\|\mathbf{u} - \mathbf{u}_h\|_{0,\Omega}$ is explained by the fact that, as shown by (4.11), it depends on the regularity of $\mathbf{u}$, $\mathbf{t}$, $\boldsymbol{\sigma}$ and $\mathbf{div}(\boldsymbol{\sigma})$. A very common way to overcome this drawback is the use of adaptive algorithms based on suitable a posteriori error estimators. This issue will be addressed in a forthcoming work.

Finally, in order to graphically illustrate the accurateness of our discrete scheme, in Figures 5.1 and 5.2 we display some components of the approximate solutions for Example 1 and 3, respectively. They all correspond to those obtained with the first mesh of each kind (triangles, quadrilaterals and hexagons, respectively) and for the polynomial degree $k = 2$

k	h	N	$\mathbf{e}(\mathbf{t})$	$\mathbf{r}(\mathbf{t})$	$\mathbf{e}_0(\boldsymbol{\sigma})$	$\mathbf{r}_0(\boldsymbol{\sigma})$	$\mathbf{e}_{\mathbf{div}}(\boldsymbol{\sigma})$	$\mathbf{r}_{\mathbf{div}}(\boldsymbol{\sigma})$	$\mathbf{e}(\mathbf{u})$	$\mathbf{r}(\mathbf{u})$	$\mathbf{e}(p)$	$\mathbf{r}(p)$	$\mathbf{e}(\boldsymbol{\sigma}^*)$	$\mathbf{r}(\boldsymbol{\sigma}^*)$
	0.0566	7601	1.43e-1	−−	3.91e-1	−−	3.79e+1	−−	3.10e-2	−−	6.49e-2	−−	1.62e-0	−−
	0.0404	14841	1.02e-1	1.00	2.80e-1	1.00	3.79e+1	0.00	2.17e-2	1.06	4.63e-2	1.01	1.15e-0	1.00
0	0.0218	50961	5.50e-2	1.00	1.51e-1	1.00	3.79e+1	0.00	1.15e-2	1.03	2.49e-2	1.00	6.22e-1	1.00
	0.0150	106409	3.80e-2	1.00	1.04e-1	1.00	3.79e+1	0.00	7.90e-3	1.01	1.72e-2	1.00	4.30e-1	1.00
	0.0118	173281	2.98e-2	1.00	8.16e-2	1.00	3.79e+1	0.00	6.18e-3	1.00	1.35e-2	1.00	3.37e-1	1.00
	0.0566	26451	3.25e-3	−−	8.80e-3	−−	1.58e-0	−−	7.35e-4	−−	7.85e-4	−−	4.49e-2	−−
	0.0404	51731	1.66e-3	2.00	4.49e-3	2.00	1.13e-0	1.00	3.72e-4	2.03	3.93e-4	2.06	2.30e-2	1.99
1	0.0218	177971	4.81e-4	2.00	1.30e-3	2.00	6.09e-1	1.00	1.07e-4	2.01	1.11e-4	2.04	6.68e-3	2.00
	0.0150	371865	2.30e-4	2.00	6.23e-4	2.00	4.21e-1	1.00	5.11e-5	2.00	5.29e-5	2.02	3.20e-3	2.00
	0.0118	605761	1.41e-4	2.00	3.82e-4	2.00	3.30e-1	1.00	3.13e-5	2.00	3.23e-5	2.02	1.96e-3	2.00
	0.0566	54051	5.95e-5	−−	1.93e-4	−−	4.83e-2	−−	1.31e-5	−−	3.24e-5	−−	2.97e-3	−−
	0.0404	105771	2.17e-5	3.00	7.06e-5	2.99	2.48e-2	1.99	4.72e-6	3.03	1.15e-5	3.08	1.11e-3	2.94
2	0.0218	364131	3.40e-6	3.00	1.10e-5	3.00	7.20e-3	2.00	7.31e-7	3.01	1.73e-6	3.06	1.76e-4	2.97
	0.0150	761025	1.12e-6	3.00	3.65e-6	3.00	3.44e-3	2.00	2.41e-7	3.00	5.64e-7	3.04	5.83e-5	2.99
	0.0118	1239841	5.40e-7	3.00	1.75e-6	3.00	2.11e-3	2.00	1.16e-7	3.00	2.69e-7	3.03	2.81e-5	2.99

Table 5.1: Example 1, history of convergence using triangles.

k	h	N	$\mathbf{e}(\mathbf{t})$	$\mathbf{r}(\mathbf{t})$	$\mathbf{e}_0(\boldsymbol{\sigma})$	$\mathbf{r_0}(\boldsymbol{\sigma})$	$\mathbf{e_{div}}(\boldsymbol{\sigma})$	$\mathbf{r_{div}}(\boldsymbol{\sigma})$	$\mathbf{e}(\mathbf{u})$	$\mathbf{r}(\mathbf{u})$	$\mathbf{e}(p)$	$\mathbf{r}(p)$	$\mathbf{e}(\boldsymbol{\sigma}^*)$	$\mathbf{r}(\boldsymbol{\sigma}^*)$
	0.0461	8716	1.18e-1	−−	3.16e-1	−−	3.79e+1	−−	2.73e-2	−−	2.84e-2	−−	1.42e-0	−−
	0.0359	14356	9.16e-2	1.00	2.46e-1	1.00	3.79e+1	0.00	2.09e-2	1.06	2.16e-2	1.08	1.10e-0	1.00
0	0.0183	54561	4.68e-2	1.00	1.26e-1	1.00	3.79e+1	0.00	1.05e-2	1.03	1.06e-2	1.06	5.64e-1	1.00
	0.0135	101281	3.43e-2	1.00	9.21e-2	1.00	3.79e+1	0.00	7.67e-3	1.01	7.80e-3	1.00	4.14e-1	1.00
	0.0101	179841	2.58e-2	1.00	6.90e-2	1.00	3.79e+1	0.00	5.74e-3	1.01	5.84e-3	1.01	3.10e-1	1.00
	0.0461	28456	2.72e-3	−−	7.56e-3	−−	1.40e-0	−−	5.81e-4	−−	1.41e-3	−−	3.56e-2	−−
	0.0359	46936	1.64e-3	2.02	4.53e-3	2.04	1.09e-0	1.00	3.50e-4	2.02	7.79e-4	2.35	2.15e-2	2.00
1	0.0183	178817	4.25e-4	2.01	1.16e-3	2.03	5.57e-1	1.00	9.12e-5	2.01	1.68e-4	2.29	5.64e-3	1.99
	0.0135	332161	2.28e-4	2.01	6.22e-4	2.02	4.09e-1	1.00	4.90e-5	2.00	8.38e-5	2.23	3.04e-3	2.00
	0.0101	590081	1.28e-4	2.01	3.48e-4	2.01	3.07e-1	1.00	2.75e-5	2.00	4.46e-5	2.19	1.71e-3	2.00
	0.0461	56771	4.28e-5	−−	1.39e-4	−−	3.57e-2	−−	8.52e-6	−−	3.33e-5	−−	1.89e-3	−−
	0.0359	93691	2.00e-5	3.03	6.46e-5	3.06	2.16e-2	2.00	4.00e-6	3.00	1.47e-5	3.24	9.09e-4	2.92
2	0.0183	357281	2.64e-6	3.02	8.56e-6	3.02	5.68e-3	1.99	5.35e-7	3.00	1.85e-6	3.09	1.24e-4	2.97
	0.0135	663841	1.04e-6	3.01	3.36e-6	3.01	3.06e-3	1.99	2.11e-7	3.00	7.07e-7	3.10	4.90e-5	3.00
	0.0101	1179521	4.36e-7	3.02	1.41e-6	3.02	1.72e-3	2.00	8.89e-8	3.00	2.92e-7	3.07	2.07e-5	3.00

Table 5.2: Example 1, history of convergence using quadrilaterals.

k	h	N	$\mathbf{e}(\mathbf{t})$	$\mathbf{r}(\mathbf{t})$	$\mathbf{e}_0(\boldsymbol{\sigma})$	$\mathbf{r_0}(\boldsymbol{\sigma})$	$\mathbf{e_{div}}(\boldsymbol{\sigma})$	$\mathbf{r_{div}}(\boldsymbol{\sigma})$	$\mathbf{e}(\mathbf{u})$	$\mathbf{r}(\mathbf{u})$	$\mathbf{e}(p)$	$\mathbf{r}(p)$	$\mathbf{e}(\boldsymbol{\sigma}^*)$	$\mathbf{r}(\boldsymbol{\sigma}^*)$
	0.0439	11262	1.24e-1	−−	3.53e-1	−−	3.79e+1	−−	2.63e-2	−−	8.67e-2	−−	1.42e-0	−−
	0.0342	18255	9.61e-2	1.04	2.70e-1	1.08	3.79e+1	0.00	2.05e-2	1.00	6.05e-2	1.44	1.11e-0	1.00
0	0.0251	33870	7.01e-2	1.02	1.95e-1	1.05	3.79e+1	0.00	1.50e-2	1.01	3.94e-2	1.39	8.12e-1	1.00
	0.0182	64243	5.04e-2	1.02	1.39e-1	1.04	3.79e+1	0.00	1.08e-2	1.00	2.55e-2	1.34	5.89e-1	1.00
	0.0132	121206	3.64e-2	1.01	9.99e-2	1.03	3.79e+1	0.00	7.86e-3	1.00	1.67e-2	1.31	4.27e-1	1.00
	0.0439	33782	2.28e-3	−−	6.27e-3	−−	1.39e-0	−−	5.01e-4	−−	9.82e-4	−−	3.07e-2	−−
	0.0342	54761	1.39e-3	1.99	3.80e-3	2.01	1.09e-0	0.99	3.04e-4	2.01	5.47e-4	2.35	1.85e-2	2.03
1	0.0251	101606	7.43e-4	2.02	2.04e-3	2.02	7.99e-1	1.00	1.63e-4	2.01	2.86e-4	2.08	1.01e-2	1.97
	0.0182	192871	3.91e-4	1.99	1.07e-3	1.99	5.80e-1	0.99	8.55e-5	2.00	1.50e-4	2.00	5.35e-3	1.96
	0.0132	363614	2.05e-4	2.00	5.61e-4	2.01	4.20e-1	1.00	4.49e-5	2.00	7.34e-5	2.22	2.81e-3	2.00
	0.0439	65059	3.60e-5	−−	1.23e-4	−−	3.20e-2	−−	6.53e-6	−−	3.65e-5	−−	1.59e-3	−−
	0.0342	105463	1.70e-5	3.01	5.74e-5	3.05	1.93e-2	2.02	3.11e-6	2.98	1.71e-5	3.05	7.85e-4	2.84
2	0.0251	195683	6.79e-6	2.96	2.30e-5	2.95	1.05e-2	1.96	1.22e-6	3.03	6.81e-6	2.97	3.06e-4	3.03
	0.0182	371577	2.59e-6	2.99	8.84e-6	2.96	5.58e-3	1.96	4.66e-7	2.98	2.60e-6	2.98	1.21e-4	2.87
	0.0132	700291	9.85e-7	3.01	3.36e-6	3.01	2.93e-3	2.00	1.77e-7	3.01	9.84e-7	3.02	4.58e-5	3.03

Table 5.3: Example 1, history of convergence using hexagons.

k	h	N	$\mathbf{e}(\mathbf{t})$	$\mathbf{r}(\mathbf{t})$	$\mathbf{e}_0(\boldsymbol{\sigma})$	$\mathbf{r_0}(\boldsymbol{\sigma})$	$\mathbf{e_{div}}(\boldsymbol{\sigma})$	$\mathbf{r_{div}}(\boldsymbol{\sigma})$	$\mathbf{e}(\mathbf{u})$	$\mathbf{r}(\mathbf{u})$	$\mathbf{e}(p)$	$\mathbf{r}(p)$	$\mathbf{e}(\boldsymbol{\sigma}^*)$	$\mathbf{r}(\boldsymbol{\sigma}^*)$
	0.0566	7601	1.26e-1	−−	1.13e-1	−−	7.17e-0	−−	2.23e-2	−−	4.60e-2	−−	4.12e-1	−−
	0.0404	14841	9.04e-2	0.98	8.00e-2	1.02	7.17e-0	0.00	1.59e-2	1.01	3.19e-2	1.09	2.94e-1	0.99
0	0.0218	50961	4.89e-2	0.99	4.28e-2	1.01	7.17e-0	0.00	8.55e-3	1.00	1.66e-2	1.05	1.59e-1	1.00
	0.0150	106409	3.39e-2	1.00	2.95e-2	1.00	7.17e-0	0.00	5.91e-3	1.00	1.14e-2	1.02	1.10e-1	1.00
	0.0118	173281	2.66e-2	1.00	2.31e-2	1.00	7.17e-0	0.00	4.63e-3	1.00	8.89e-3	1.02	8.59e-2	1.00
	0.0566	26451	3.16e-3	−−	3.74e-3	−−	3.98e-1	−−	4.47e-4	−−	2.06e-3	−−	1.86e-2	−−
	0.0404	51731	1.66e-3	1.92	1.93e-3	1.97	2.85e-1	1.00	2.28e-4	2.01	1.05e-3	2.00	9.49e-3	2.00
1	0.0218	177971	4.93e-4	1.96	5.65e-4	1.98	1.53e-1	1.00	6.59e-5	2.00	3.04e-4	2.00	2.76e-3	2.00
	0.0150	371865	2.37e-4	1.98	2.71e-4	1.99	1.06e-1	1.00	3.15e-5	2.00	1.45e-4	2.00	1.32e-3	2.00
	0.0118	605761	1.46e-4	1.99	1.66e-4	1.99	8.31e-2	1.00	1.93e-5	2.00	8.92e-5	2.00	8.09e-4	2.00
	0.0566	54051	6.53e-5	−−	1.19e-4	−−	2.05e-2	−−	5.06e-6	−−	7.63e-5	−−	6.56e-4	−−
	0.0404	105771	2.37e-5	3.01	4.34e-5	3.00	1.05e-2	1.99	1.82e-6	3.04	2.78e-5	3.00	2.39e-4	3.00
2	0.0218	364131	3.71e-6	3.00	6.77e-6	3.00	3.04e-3	2.00	2.80e-7	3.02	4.34e-6	3.00	3.74e-5	3.00
	0.0150	761025	1.23e-6	3.00	2.24e-6	3.00	1.45e-3	2.00	9.25e-8	3.01	1.43e-6	3.00	1.24e-5	3.00
	0.0118	1239841	5.90e-7	3.00	1.08e-6	3.00	8.92e-4	2.00	4.44e-8	3.00	6.88e-7	3.00	5.94e-6	3.00

Table 5.4: Example 2, history of convergence using triangles.

k	h	N	$\mathbf{e(t)}$	$\mathbf{r(t)}$	$\mathbf{e}_0(\boldsymbol{\sigma})$	$\mathbf{r_0}(\boldsymbol{\sigma})$	$\mathbf{e_{div}}(\boldsymbol{\sigma})$	$\mathbf{r_{div}}(\boldsymbol{\sigma})$	$\mathbf{e(u)}$	$\mathbf{r(u)}$	$\mathbf{e}(p)$	$\mathbf{r}(p)$	$\mathbf{e}(\boldsymbol{\sigma}^*)$	$\mathbf{r}(\boldsymbol{\sigma}^*)$
	0.0461	8716	7.05e-2	−−	7.54e-2	−−	7.17e-0	−−	2.04e-2	−−	3.89e-2	−−	3.54e-1	−−
	0.0359	14356	5.45e-2	1.02	5.80e-2	1.04	7.17e-0	0.00	1.58e-2	1.00	2.98e-2	1.05	2.75e-1	1.00
0	0.0183	54561	2.76e-2	1.01	2.93e-2	1.02	7.17e-0	0.00	8.09e-3	1.00	1.50e-2	1.03	1.41e-1	1.00
	0.0135	101281	2.02e-2	1.01	2.14e-2	1.01	7.17e-0	0.00	5.93e-3	1.00	1.09e-2	1.01	1.03e-1	1.00
	0.0101	179841	1.52e-2	1.00	1.60e-2	1.00	7.17e-0	0.00	4.45e-3	1.00	8.18e-3	1.01	7.74e-2	1.00
	0.0461	28456	1.01e-3	−−	2.41e-3	−−	3.48e-1	−−	2.87e-4	−−	1.63e-3	−−	1.46e-2	−−
	0.0359	46936	6.11e-4	1.98	1.46e-3	2.00	2.71e-1	1.00	1.73e-4	2.00	9.89e-4	2.00	8.87e-3	1.99
1	0.0183	178817	1.58e-4	2.02	3.82e-4	2.00	1.39e-1	1.00	4.53e-5	2.00	2.59e-4	2.00	2.32e-3	2.00
	0.0135	332161	8.52e-5	2.00	2.05e-4	2.00	1.02e-1	1.00	2.44e-5	2.00	1.39e-4	2.00	1.25e-3	2.00
	0.0101	590081	4.78e-5	2.01	1.15e-4	2.00	7.63e-2	1.00	1.37e-5	2.00	7.83e-5	2.00	7.02e-4	2.00
	0.0461	56771	1.19e-5	−−	6.99e-5	−−	1.48e-2	−−	2.78e-6	−−	4.90e-5	−−	4.31e-4	−−
	0.0359	93691	5.58e-6	3.01	3.28e-5	3.01	8.96e-3	2.00	1.30e-6	3.01	2.30e-5	3.01	2.03e-4	3.00
2	0.0183	357281	7.35e-7	3.02	4.35e-6	3.01	2.34e-3	2.00	1.74e-7	3.00	3.05e-6	3.01	2.72e-5	3.00
	0.0135	663841	2.90e-7	2.99	1.71e-6	3.00	1.26e-3	2.00	6.85e-8	3.01	1.20e-6	3.00	1.07e-5	3.00
	0.0101	1179521	1.22e-7	3.01	7.22e-7	3.00	7.08e-4	2.00	2.89e-8	3.00	5.07e-7	3.00	4.52e-6	3.00

Table 5.5: Example 2, history of convergence using quadrilaterals.

k	h	N	$\mathbf{e(t)}$	$\mathbf{r(t)}$	$\mathbf{e}_0(\boldsymbol{\sigma})$	$\mathbf{r_0}(\boldsymbol{\sigma})$	$\mathbf{e_{div}}(\boldsymbol{\sigma})$	$\mathbf{r_{div}}(\boldsymbol{\sigma})$	$\mathbf{e(u)}$	$\mathbf{r(u)}$	$\mathbf{e}(p)$	$\mathbf{r}(p)$	$\mathbf{e}(\boldsymbol{\sigma}^*)$	$\mathbf{r}(\boldsymbol{\sigma}^*)$
	0.0439	11262	6.54e-2	−−	7.16e-2	−−	7.17e-0	−−	1.93e-2	−−	3.75e-2	−−	3.51e-1	−−
	0.0342	18255	5.11e-2	0.99	5.58e-2	1.00	7.17e-0	0.00	1.51e-2	0.99	2.92e-2	1.01	2.74e-1	1.00
0	0.0251	33870	3.74e-2	1.00	4.08e-2	1.00	7.17e-0	0.00	1.11e-2	1.00	2.14e-2	1.00	2.01e-1	1.00
	0.0182	64243	2.72e-2	0.99	2.96e-2	0.99	7.17e-0	0.00	8.06e-3	0.99	1.55e-2	1.00	1.46e-1	0.99
	0.0132	121206	1.98e-2	0.99	2.15e-2	1.00	7.17e-0	0.00	5.85e-3	0.99	1.12e-2	1.00	1.06e-1	1.00
	0.0439	33782	8.53e-4	−−	2.06e-3	−−	3.46e-1	−−	2.61e-4	−−	1.40e-3	−−	1.25e-2	−−
	0.0342	54761	5.17e-4	2.01	1.25e-3	2.00	2.70e-1	1.00	1.60e-4	1.98	8.52e-4	2.00	7.68e-3	1.96
1	0.0251	101606	2.77e-4	2.01	6.74e-4	2.00	1.98e-1	1.00	8.57e-5	2.01	4.59e-4	2.00	4.13e-3	2.00
	0.0182	192871	1.46e-4	1.99	3.56e-4	1.98	1.44e-1	0.99	4.53e-5	1.97	2.42e-4	1.98	2.17e-3	1.99
	0.0132	363614	7.66e-5	2.00	1.87e-4	2.00	1.04e-1	1.00	2.39e-5	1.99	1.27e-4	2.00	1.14e-3	2.00
	0.0439	65059	2.42e-5	−−	6.00e-5	−−	1.31e-2	−−	2.31e-6	−−	4.03e-5	−−	3.32e-4	−−
	0.0342	105463	1.15e-5	2.98	2.89e-5	2.94	8.02e-3	1.96	1.09e-6	3.01	1.94e-5	2.93	1.57e-4	3.00
2	0.0251	195683	4.58e-6	2.97	1.14e-5	3.00	4.31e-3	2.00	4.27e-7	3.02	7.66e-6	3.00	6.19e-5	3.00
	0.0182	371577	1.75e-6	2.99	4.35e-6	2.98	2.27e-3	1.99	1.64e-7	2.97	2.92e-6	2.98	2.37e-5	2.98
	0.0132	700291	6.68e-7	2.99	1.65e-6	3.01	1.19e-3	2.00	6.26e-8	2.99	1.11e-6	3.01	9.03e-6	3.00

Table 5.6: Example 2, history of convergence using hexagons.

k	h	N	$\mathbf{e(t)}$	$\mathbf{r(t)}$	$\mathbf{e}_0(\boldsymbol{\sigma})$	$\mathbf{r_0}(\boldsymbol{\sigma})$	$\mathbf{e_{div}}(\boldsymbol{\sigma})$	$\mathbf{r_{div}}(\boldsymbol{\sigma})$	$\mathbf{e(u)}$	$\mathbf{r(u)}$	$\mathbf{e}(p)$	$\mathbf{r}(p)$	$\mathbf{e}(\boldsymbol{\sigma}^*)$	$\mathbf{r}(\boldsymbol{\sigma}^*)$
	0.0101	7169	3.97e-2	−−	5.43e-2	−−	1.56e-0	−−	7.75e-3	−−	2.71e-2	−−	1.15e-1	−−
	0.0673	16045	2.66e-2	0.98	3.58e-2	1.02	1.56e-0	0.00	5.08e-3	1.04	1.76e-2	1.06	8.48e-2	0.74
0	0.0372	52289	1.48e-2	0.99	1.97e-2	1.01	1.56e-0	0.00	2.78e-3	1.02	9.53e-3	1.03	5.52e-2	0.72
	0.0253	113345	1.00e-2	1.00	1.33e-2	1.01	1.56e-0	0.00	1.88e-3	1.01	6.43e-3	1.02	4.19e-2	0.71
	0.0186	208545	7.40e-3	1.00	9.80e-3	1.00	1.56e-0	0.00	1.39e-3	1.00	4.73e-3	1.01	3.39e-2	0.70
	0.0101	24921	9.36e-4	−−	1.55e-3	−−	1.06e-1	−−	2.43e-4	−−	9.02e-4	−−	3.38e-2	−−
	0.0673	55903	4.52e-4	1.79	7.83e-4	1.69	8.08e-1	0.68	1.08e-4	2.01	4.62e-4	1.65	2.57e-2	0.67
1	0.0372	182553	1.58e-4	1.77	2.89e-4	1.68	5.41e-2	0.68	3.28e-5	2.00	1.73e-4	1.65	1.73e-2	0.67
	0.0253	396033	8.04e-5	1.75	1.51e-4	1.68	4.17e-2	0.67	1.51e-5	2.00	9.12e-5	1.66	1.34e-2	0.67
	0.0186	728993	4.73e-5	1.74	9.03e-5	1.68	3.39e-2	0.67	8.18e-6	2.00	5.49e-5	1.66	1.09e-2	0.67
	0.0101	50905	6.23e-5	−−	2.78e-4	−−	3.96e-2	−−	6.02e-6	−−	1.92e-4	−−	1.93e-2	−−
	0.0673	114283	3.15e-5	1.68	1.41e-4	1.67	3.02e-2	0.67	1.92e-6	2.82	9.75e-5	1.67	1.48e-2	0.67
2	0.0372	373465	1.17e-5	1.67	5.26e-5	1.67	2.03e-2	0.67	3.67e-7	2.79	3.63e-5	1.67	9.93e-3	0.67
	0.0253	810433	6.13e-6	1.67	2.76e-5	1.67	1.57e-2	0.67	1.26e-7	2.76	1.90e-5	1.67	7.67e-3	0.67
	0.0186	1492033	3.68e-6	1.67	1.66e-5	1.67	1.28e-2	0.67	5.43e-8	2.75	1.14e-5	1.67	6.26e-3	0.67

Table 5.7: Example 3, history of convergence using triangles.

k	h	N	$\mathbf{e}(\mathbf{t})$	$\mathbf{r}(\mathbf{t})$	$\mathbf{e}_0(\boldsymbol{\sigma})$	$\mathbf{r_0}(\boldsymbol{\sigma})$	$\mathbf{e_{div}}(\boldsymbol{\sigma})$	$\mathbf{r_{div}}(\boldsymbol{\sigma})$	$\mathbf{e}(\mathbf{u})$	$\mathbf{r}(\mathbf{u})$	$\mathbf{e}(p)$	$\mathbf{r}(p)$	$\mathbf{e}(\boldsymbol{\sigma}^*)$	$\mathbf{r}(\boldsymbol{\sigma}^*)$
	0.0907	8561	2.22e-2	−−	3.85e-2	−−	1.56e-0	−−	6.15e-3	−−	2.28e-2	−−	1.09e-1	−−
	0.0725	13326	1.77e-2	1.02	3.03e-2	1.07	1.56e-0	0.00	4.87e-3	1.05	1.78e-2	1.09	9.42e-2	0.66
0	0.0363	52901	8.74e-3	1.02	1.47e-2	1.05	1.56e-0	0.00	2.38e-3	1.03	8.55e-3	1.06	6.13e-2	0.62
	0.0245	115589	5.88e-3	1.01	9.84e-3	1.02	1.56e-0	0.00	1.60e-3	1.02	5.73e-3	1.02	4.47e-2	0.80
	0.0191	190286	4.58e-3	1.00	7.63e-3	1.02	1.56e-0	0.00	1.24e-3	1.01	4.44e-3	1.02	3.82e-2	0.63
	0.0907	27921	5.40e-4	−−	1.33e-3	−−	1.06e-1	−−	1.72e-4	−−	8.71e-4	−−	4.23e-2	−−
	0.0725	43526	3.78e-4	1.59	9.29e-4	1.60	9.16e-2	0.66	1.12e-4	1.93	6.07e-4	1.62	3.67e-2	0.64
1	0.0363	173301	1.09e-4	1.79	3.31e-4	1.49	6.01e-2	0.61	2.79e-5	2.00	2.22e-4	1.45	2.55e-2	0.52
	0.0245	379029	5.08e-5	1.96	1.65e-4	1.78	4.54e-2	0.71	1.27e-5	2.01	1.12e-4	1.76	1.83e-2	0.84
	0.0191	624246	3.36e-5	1.66	1.05e-4	1.80	3.86e-2	0.66	7.69e-6	2.00	7.09e-5	1.82	1.58e-2	0.60
	0.0907	55681	9.07e-5	−−	3.37e-4	−−	4.58e-2	−−	4.16e-6	−−	2.29e-4	−−	2.90e-2	−−
	0.0725	86851	6.26e-5	1.66	2.32e-4	1.67	3.93e-2	0.69	2.04e-6	3.20	1.58e-4	1.67	2.52e-2	0.64
2	0.0363	346201	2.56e-5	1.29	9.17e-5	1.34	2.73e-2	0.53	3.60e-7	2.50	6.23e-5	1.34	1.81e-2	0.48
	0.0245	757465	1.30e-5	1.74	4.64e-5	1.74	2.00e-2	0.78	1.15e-7	2.90	3.15e-5	1.74	1.29e-2	0.86
	0.0191	1247731	7.87e-6	2.00	2.68e-5	2.19	1.70e-2	0.68	5.58e-8	2.93	1.81e-5	2.21	1.06e-2	0.77

Table 5.8: Example 3, history of convergence using quadrilaterals.

k	h	N	$\mathbf{e}(\mathbf{t})$	$\mathbf{r}(\mathbf{t})$	$\mathbf{e}_0(\boldsymbol{\sigma})$	$\mathbf{r_0}(\boldsymbol{\sigma})$	$\mathbf{e_{div}}(\boldsymbol{\sigma})$	$\mathbf{r_{div}}(\boldsymbol{\sigma})$	$\mathbf{e}(\mathbf{u})$	$\mathbf{r}(\mathbf{u})$	$\mathbf{e}(p)$	$\mathbf{r}(p)$	$\mathbf{e}(\boldsymbol{\sigma}^*)$	$\mathbf{r}(\boldsymbol{\sigma}^*)$
	0.0866	8382	2.26e-2	−−	4.02e-2	−−	1.56e-0	−−	6.62e-3	−−	2.41e-2	−−	1.18e-1	−−
	0.0462	28668	1.20e-2	1.01	2.10e-2	1.03	1.56e-0	0.00	3.49e-3	1.02	1.25e-2	1.04	7.73e-2	0.68
0	0.0315	61050	8.13e-3	1.02	1.42e-2	1.02	1.56e-0	0.00	2.38e-3	1.00	8.48e-3	1.02	5.98e-2	0.67
	0.0247	98868	6.38e-3	1.00	1.11e-2	1.02	1.56e-0	0.00	1.87e-3	1.00	6.63e-3	1.02	5.16e-2	0.61
	0.0204	145758	5.25e-3	1.01	9.16e-3	1.01	1.56e-0	0.00	1.54e-3	0.99	5.45e-3	1.01	4.60e-2	0.58
	0.0866	25142	5.93e-4	−−	1.50e-3	−−	1.15e-1	−−	1.86e-4	−−	9.84e-4	−−	4.87e-2	−−
	0.0462	86000	1.84e-4	1.86	5.45e-4	1.61	7.66e-2	0.65	5.38e-5	1.97	3.65e-4	1.58	3.24e-2	0.65
1	0.0315	183146	9.66e-5	1.68	2.96e-4	1.60	5.98e-2	0.65	2.52e-5	1.98	1.99e-4	1.59	2.63e-2	0.54
	0.0247	296600	6.30e-5	1.77	2.02e-4	1.59	5.16e-2	0.61	1.55e-5	2.01	1.36e-4	1.57	2.26e.2	0.62
	0.0204	437270	4.48e-5	1.76	1.49e-4	1.55	4.52e-2	0.68	1.06e-5	1.99	1.01e-4	1.53	2.00e-2	0.63
	0.0866	48419	9.62e-5	−−	4.32e-4	−−	5.08e-2	−−	4.09e-6	−−	2.98e-4	−−	3.35e-2	−−
	0.0462	165627	3.32e-5	1.69	1.58e-4	1.60	3.41e-2	0.63	7.64e-7	2.67	1.09e-4	1.59	2.31e-2	0.59
2	0.0315	352723	2.01e-5	1.31	9.18e-5	1.42	2.73e-2	0.58	2.65e-7	2.77	6.33e-5	1.43	1.85e-2	0.58
	0.0247	571227	1.24e-5	2.00	6.32e-5	1.55	2.36e-2	0.59	1.50e-7	2.34	4.38e-5	1.53	1.61e-2	0.56
	0.0204	842174	9.85e-6	1.19	4.76e-5	1.46	2.10e-2	0.61	8.41e-8	3.00	3.29e-5	1.47	1.44e-2	0.58

Table 5.9: Example 3, history of convergence using hexagons.

References

[1] B. Ahmad, A. Alsaedi, F. Brezzi, L. D. Marini, and A. Russo, *Equivalent projectors for virtual element methods*, Comput. Math. Appl., 66 (2013), pp. 376–391.

[2] P. F. Antonietti, L. Beirão da Veiga, D. Mora, and M. Verani, *A stream virtual element formulation of the Stokes problem on polygonal meshe*, SIAM J. Numer. Anal., 52 (2017), pp. 386–404.

[3] L. Beirão da Veiga, F. Brezzi, A. Cangiani, G. Manzini, L. D. Marini, and A. Russo, *Basic principles of virtual element methods*, Math. Models Methods Appl. Sci., 23 (2013), pp. 199–214.

[4] L. Beirão da Veiga, F. Brezzi, L. D. Marini, and A. Russo, *$H(\mathrm{div})$ and $H(\mathbf{curl})$-conforming virtual element method*, Numer. Math., 133 (2016), pp. 303–332.

[5] ——, *Mixed virtual element methods for general second order elliptic problems on polygonal meshes*, ESAIM Math. Model. Numer. Anal., 50 (2016), pp. 727–747.

[6] L. Beirão da Veiga, C. Lovadina, and G. Vacca, *Divergence free virtual elements for the Stokes problem on polygonal meshes*, ESAIM Math. Model. Numer. Anal., 51 (2017), pp. 509–535.

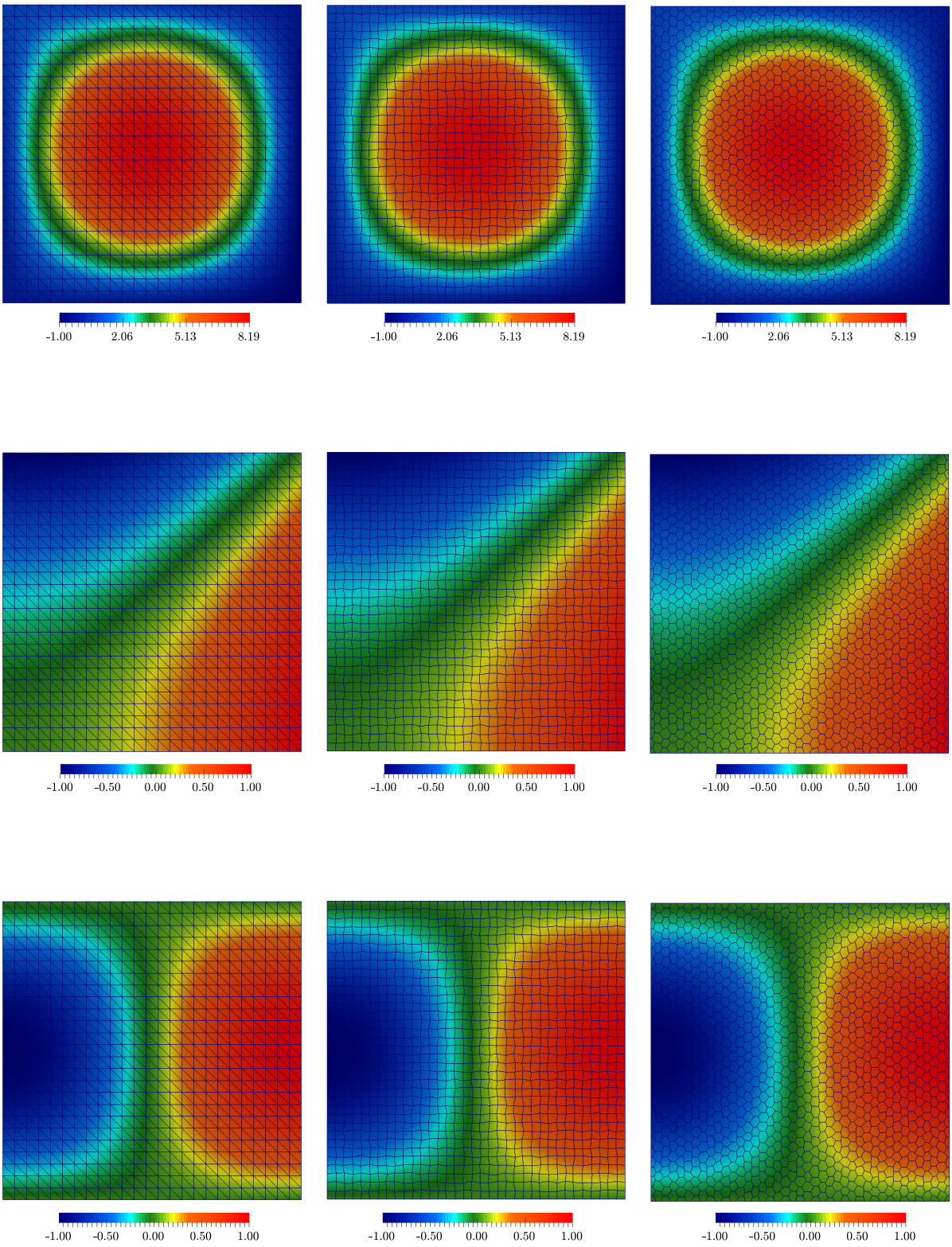

Figure 5.1: Example 1, $\sigma_{h,11}$ (top), p_h (middle) and $u_{h,1}$ (bottom).

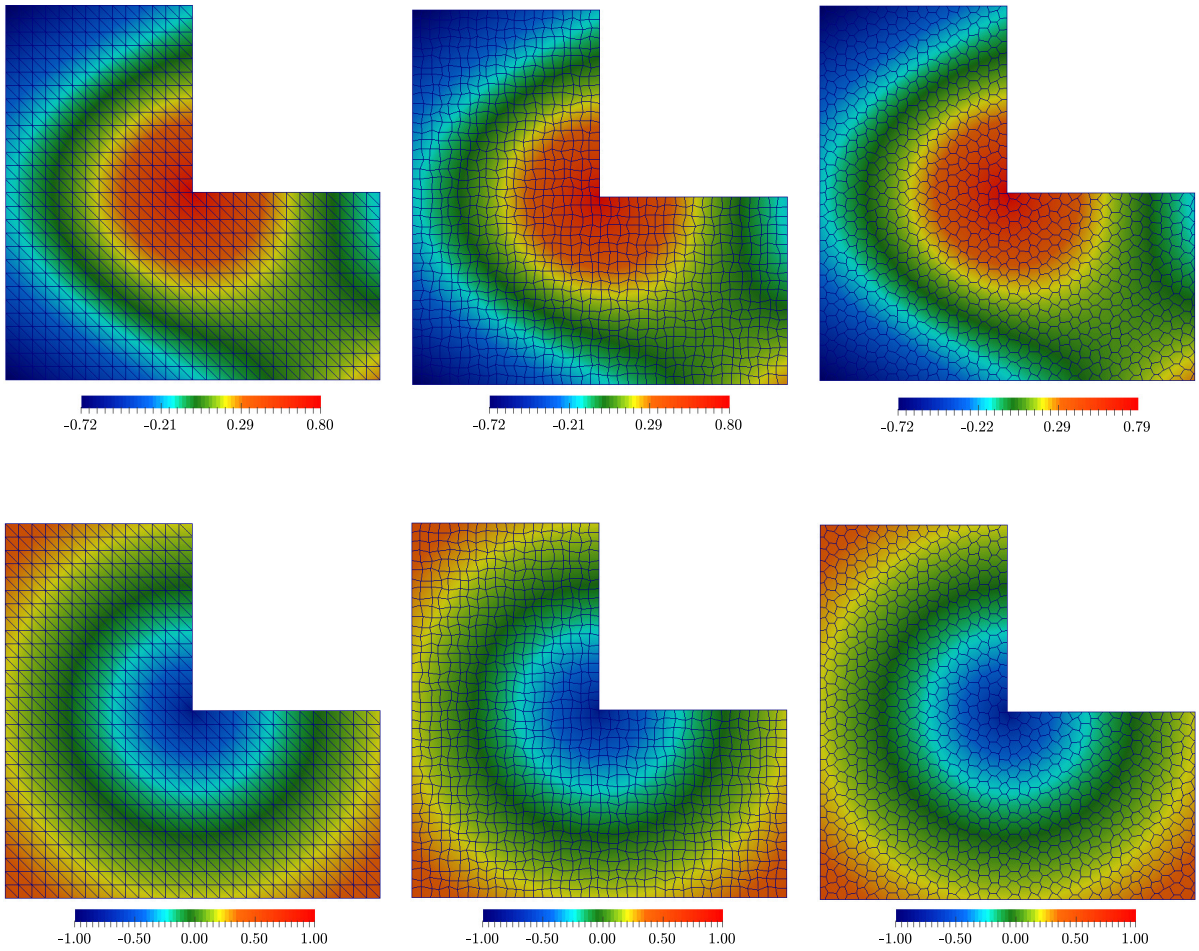

Figure 5.2: Example 3, $\sigma_{h,22}$ (top) and p_h (bottom).

[7] ——, *Virtual elements for the Navier-Stokes problem on polygonal meshes*, arXiv:1703.00437v2 [math.NA], (2017).

[8] F. Brezzi, R. S. Falk, and L. D. Marini, *Basic principles of mixed virtual element methods*, ESAIM Math. Model. Numer. Anal., 48 (2014), pp. 1227–1240.

[9] F. Brezzi and M. Fortin, *Mixed and Hybrid Finite Element Methods*, Springer Verlag, New York, 1991.

[10] E. Cáceres and G. N. Gatica, *A mixed virtual element method for the pseudostress-velocity formulation of the Stokes problem*, IMA J. Numer. Anal., 37 (2017), pp. 296–331.

[11] E. Cáceres, G. N. Gatica, and F. A. Sequeira, *A mixed virtual element method for quasi-Newtonian Stokes flows*, SIAM J. Numer. Anal., to appear.

[12] ——, *A mixed virtual element method for the Brinkman problem*, Math. Models Methods Appl. Sci., 27 (2017), pp. 707–743.

[13] J. Camaño, G. N. Gatica, R. Oyarzúa, and R. Ruiz-Baier, *An augmented stress-based mixed finite element method for the steady state Navier-Stokes equations with nonlinear viscosity*, Numer. Methods Partial Differential Equations, 33 (2017), pp. 1692–1725.

[14] J. Camaño, G. N. Gatica, R. Oyarzúa, and G. Tierra, *An augmented mixed finite element method for the Navier-Stokes equations with variable viscosity*, SIAM J. Numer. Anal., 54 (2016), pp. 1069–1092.

[15] J. Camaño, R. Oyarzúa, and G. Tierra, *Analysis of an augmented mixed-FEM for the Navier-Stokes problem*, Math. Comp., 86 (2017), pp. 589–615.

[16] A. Cangiani, V. Gyrya, and G. Manzini, *The nonconforming virtual element method for the Stokes equations*, SIAM J. Numer. Anal., 54 (2016), pp. 3411–3435.

[17] G. N. Gatica, L. F. Gatica, and A. Márquez, *Analysis of a pseudostress-based mixed finite element method for the Brinkman model of porous media flow*, Numer. Math., 126 (2014), pp. 635–677.

[18] G. N. Gatica, L. F. Gatica, and F. A. Sequeira, *Analysis of an augmented pseudostress-based mixed formulation for a nonlinear Brinkman model of porous media flow*, Comput. Methods Appl. Mech. Engrg., 289 (2015), pp. 104–130.

[19] ——, *A $\mathbb{RT}_k - \mathbf{P}_k$ approximation for linear elasticity yielding a broken $\mathbb{H}(\mathbf{div})$ convergent post-processed stress*, Appl. Math. Lett., 49 (2015), pp. 133–140.

[20] ——, *A priori and a posteriori error analyses of a pseudostress-based mixed formulation for linear elasticity*, Comput. Math. Appl., 71 (2016), pp. 585–614.

[21] G. N. Gatica, M. González, and S. Meddahi, *A low-order mixed finite element method for a class of quasi-Newtonian Stokes flows. I: a priori error analysis*, Comput. Methods Appl. Mech. Engrg., 193 (2004), pp. 881–892.

[22] G. N. Gatica, A. Márquez, and M. A. Sánchez, *A priori and a posteriori error analyses of a velocity-pseudostress formulation for a class of quasi-Newtonian Stokes flows*, Comput. Methods Appl. Mech. Engrg., 200 (2011), pp. 1619–1636.

[23] G. N. Gatica, M. Munar, and F. A. Sequeira, *A mixed virtual element method for the Navier-Stokes equations*, Preprint 2017-23, Centro de Investigación en Ingeniería Matemática, Universidad de Concepción, (2017). [available at `http://www.ci2ma.udec.cl/publicaciones/prepublicaciones/`].

[24] G. N. Gatica and F. A. Sequeira, *Analysis of an augmented HDG method for a class of quasi-Newtonian Stokes flows*, J. Sci. Comput., 65 (2015), pp. 1270–1308.

[25] ——, *A priori and a posteriori error analyses of an augmented HDG method for a class of quasi-Newtonian Stokes flows*, J. Sci. Comput., 69 (2016), pp. 1192–1250.

[26] J. S. Howell, *Dual-mixed finite element approximation of Stokes and nonlinear Stokes problems using trace-free velocity gradients*, J. Comput. Appl. Math., 231 (2009), pp. 780–792.

[27] A. F. D. Loula and J. N. C. Guerreiro, *Finite element analysis of nonlinear creeping flows*, Comput. Methods Appl. Mech. Engrg., 79 (1990), pp. 87–109.

[28] D. Sandri, *Sur l'approximation numérique des écoulements quasi-newtoniens dont la viscosité suit la loi puissance ou la loi de Carreau*, RAIRO Modél. Math. Anal. Numér. Anal., 27 (1993), pp. 131–155.

[29] E. Zeidler, *Nonlinear Functional Analysis and its Applications II/B: Nonlinear Monotone Operators*, Springer-Verlag New York, 1990.

Centro de Investigación en Ingeniería Matemática (CI^{2}MA)

PRE-PUBLICACIONES 2017

2017-21 Sergio Caucao, Gabriel N. Gatica, Ricardo Oyarzúa: *Analysis of an augmented fully-mixed formulation for the non-isothermal Oldroyd-Stokes problem*

2017-22 Rolando Biscay, Joaquin Fernández, Carlos M. Mora: *Numerical solution of stochastic master equations using stochastic interacting wave functions*

2017-23 Gabriel N. Gatica, Mauricio Munar, Filander A. Sequeira: *A mixed virtual element method for the Navier-Stokes equations*

2017-24 Nicolas Barnafi, Gabriel N. Gatica, Daniel E. Hurtado: *Primal and mixed finite element methods for deformable image registration problems*

2017-25 Sergio Caucao, Gabriel N. Gatica, Ricardo Oyarzúa: *A posteriori error analysis of an augmented fully-mixed formulation for the non-isothermal Oldroyd-Stokes problem*

2017-26 Raimund Bürger, Stefan Diehl, María Carmen Martí: *A conservation law with multiply discontinuous flux modelling a flotation column*

2017-27 Antonio Baeza, Raimund Bürger, Pep Mulet, David Zorío: *Central WENO schemes through a global average weight*

2017-28 Rodolfo Araya, Manuel Solano, Patrick Vega: *Analysis of an adaptive HDG method for the Brinkman problem*

2017-29 Sergio Caucao, Marco Discacciati, Gabriel N. Gatica, Ricardo Oyarzúa: *A conforming mixed finite element method for the Navier-Stokes/Darcy-Forchheimer coupled problem*

2017-30 Tonatiuh Sanchez-Vizuet, Manuel Solano: *A Hybridizable Discontinuous Galerkin solver for the Grad-Shafranov equation*

2017-31 David Mora, Gonzalo Rivera: *A priori and a posteriori error estimates for a virtual element spectral analysis for the elasticity equations*

2017-32 Gabriel N. Gatica, Mauricio Munar, Filander A. Sequeira: *A mixed virtual element method for a nonlinear Brinkman model of porous media flow*

Para obtener copias de las Pre-Publicaciones, escribir o llamar a: Director, Centro de Investigación en Ingeniería Matemática, Universidad de Concepción, Casilla 160-C, Concepción, Chile, Tel.: 41-2661324, o bien, visitar la página web del centro: `http://www.ci2ma.udec.cl`







Centro de Investigación en
Ingeniería Matemática (CI²MA)
Universidad de Concepción

Casilla 160-C, Concepción, Chile
Tel.: 56-41-2661324/2661554/2661316
http://www.ci2ma.udec.cl